In vitro anticancer activity of novel organometallic gold and ruthenium complexes

Meshack Kekana

14034388

10 April 2020

Submitted in partial fulfilment of the degree:
M.Sc. Biochemistry
Specialization Biochemistry
Department of Biochemistry Genetics and Microbiology
University of Pretoria

DECLARATION OF ORIGINALITY UNIVERSITY OF PRETORIA

The department of Biochemistry places great emphasis on integrity and ethical conduct in the preparation of all written work submitted for academic evaluation.

While academic staff teaches you about referencing techniques and how to avoid plagiarism, you too have a responsibility in this regard. If you are at any stage uncertain as to what is required, you should speak to your lecturer before any written work is submitted.

You are guilty of plagiarism if you copy something from another author's work (e.g. a book, an article or a website) without acknowledging the source and pass it off as your own. In effect, you are stealing something that belongs to someone else. This is not only the case when you copy work word-for-word (verbatim), but also when you submit someone else's work in a slightly altered form (paraphrase) or use a line of argument without acknowledging it. You are not allowed to use work previously produced by another student. You are also not allowed to let anybody copy your work with the intention of passing it off as his/her work.

Students who commit plagiarism will not be given any credit for plagiarised work. The matter may also be referred to the Disciplinary Committee (Students) for a ruling. Plagiarism is regarded as a serious contravention of the University's rules and can lead to expulsion from the University.

The declaration which follows must accompany all written work submitted while you are a student of the Department of Biochemistry. No written work will be accepted unless the declaration has been completed and attached.

Full names of student: Meshack Kekana

Student Number: 14034388

The topic of work: In vitro anti-cancer activity of novel organometallic gold and ruthenium complexes.

Declaration

1. I understand what plagiarism is and am aware of the University's policy in this regard.

2. I declare that this ……dissertation…… (E.g. essay, report, project, assignment, dissertation, thesis, etc.) is my own original work. Where other people's work has been used (either from a printed source, Internet or any other source), this has been properly acknowledged and referenced in accordance with departmental requirements.

3. I have not used work previously produced by another student or any other person to hand in as my own.

4. I have not allowed, and will not allow, anyone, to copy my work with the intention of passing it off as his or her own work.

SIGNATURE 

Summary

In vitro anticancer activity of novel organometallic gold and ruthenium complexes

By

Meshack Kekana

Supervisor: **Dr N H Gama**

Co-supervisor**: Prof. D Meyer**

Department: **Biochemistry Genetics Microbiology**

Division: **Biochemistry**

Degree: **M.Sc. Biochemistry**

Background: Cancer is a genetic disorder characterized by an uncontrollable cell growth caused by a malfunction in the genes responsible for controlling the growth and division phases of the cell cycle. The disease can either be hereditary or may develop due to carcinogen exposure. During cancer development, there is an increase in cellular oxidative stress, resulting from an imbalance in the production of reactive oxygen species (ROS) and the cell's antioxidant defences. This plays a significant role in the development of cancer. Furthermore, normal or programmed cell death (apoptosis) is evaded, resulting in continual cell growth. Over the past century, metal-based drugs have been investigated as therapeutic agents and the platinum drugs cisplatin and carboplatin are the two most widely used metal-based chemotherapeutic agents. In addition to platinum complexes, other metals including ruthenium and gold-based complexes have been shown to have antiproliferative activity against melanoma cells.

Methods: This study aimed to investigate the anti-cancer activity of fourteen novel gold and ruthenium metal complexes. The gold complexes were derived from two parent compounds (**AE215** and **AE207**) and our research group previously showed that complex **AE215** had anti-HIV activity. Therefore, different complexes were synthesized using the parent complexes as a starting point and these complexes were either glycosylated (**G3** and **G4**) acetylated (**G5** and **G6**), or thiolated (**G8** and **G8**) gold complexes; while the ruthenium complexes were either just the ligand (**R1**), monometallic (**R2**), bimetallic trans-(**R3**) and cis-conformation (**R4**). Using **Cisplatin** as a control, the differences in the anticancer activity of these different complexes were investigated and the 50% cytotoxic concentrations (CC_{50}) were obtained by treatments at concentrations ranging from 0.78 to 50 µM on the cancer cell lines. These cancer cell lines were **HeLa**, **HepG2** and **U937** cells; and the mammalian **Vero** cell line was used to determine the selectivity of each complex. The complexes were further investigated for their antioxidant activity using the DPPH and NO assays and the effects of the complexes on the induction of apoptosis was investigated through flow cytometry using propidium iodide and Annexin V at CC_{50} and twice the CC_{50}. Finally,

the drug-likeness of the complexes was determined using Molinspiration to determine if the complexes complied with Lipinski's rule of five for potential drug candidates.

Results: Three of the gold complexes (**AE215**, **G3**, and **G5**) and two of the ruthenium complexes (**R2** and **R3**) were cytotoxic and selective to the HeLa cells where they had CC_{50}< 7 µM and SI> 1. **AE215**, **G3**, **G5**, **R2,** and **R3** were more cytotoxic than cisplatin which had a CC_{50} of 9.92 µM and SI of 1.03. The gold complex **G8** and all four ruthenium complexes were cytotoxic to HepG2 cells with CC_{50}< 9 µM and SI> 1. These complexes were more cytotoxic than cisplatin, which had a CC_{50} of 26.74 µM and an SI of 0.38 for this HepG2 cell line. Three of the gold complexes (**AE 215, G3**, and **G8**) and the ruthenium complex **R3** were cytotoxic to U937 cells with CC_{50}< 9 µM and an SI> 1. None of the gold complexes showed DPPH-scavenging ability whereas the ruthenium complexes **R2**, **R3**, and **R4** had slight DPPH-scavenging activity above 20%. All complexes were able to inhibit NO production, where complexes **G5**, **G6**, **G8**, **R2,** and **R3** were able to decrease NO concentration from 80 µM (untreated cells) to below 40 µM when tested on HeLa cells. Complexes **R3** and **R4** were able to decrease NO concentration from 97 µM (untreated cells) to just below 30 µM, and this reduction was better than that of Vitamin C which decreased NO concentration to just above 32 µM when tested on HepG2 cells. Complexes **R2**, **R3**, and **R4** were able to decrease NO production from just above 93 µM (untreated cells) to just above 23 µM at CC_{50}. All of the complexes were able to induce apoptosis. Further investigation on the drug-likeness of the complexes showed that only the two gold complexes (**AE215** and **AE207**) abided to all five of Lipinski's rules of oral bioavailability.

Conclusion: The metal complexes presented herein display the potential of being developed into improved anticancer therapies. The complexes were able to inhibit cancer cell progression when tested on HeLa, U937, and HepG2 cancer cells and were more selective than cisplatin, which is currently available on the market. The complexes not only inhibited cancer cell growth, but complexes like **R2**, **R3**, and **R4** also had antioxidant activity, showing the added benefits of these complexes. The modifications and different conformations of these complexes showed that some complexes were only active against one cancer cell type, while other complexes showed activity against all the tested cancer cells.

Acknowledgements

- Jesus Christ for making it all possible
- My mother, Elizabeth Kekana, for the endless support
- My aunt and the rest of the family for financial support
- The NRF for funding the project
- Prof Meyer and Dr Gama for giving me the opportunity
- Sonya, Sandra, and Saronda for making life in the lab very easy and manageable
- My lab partners, Tumi, Brandon, and Nomthi for the friendship and support
- To Sabela Ramafoko for making me believe in myself when I was doubtful
- Mr Court and Mr Jonathan for the support in the office
- Amogelang Makamedi for the support throughout the project
- Tyrese Rikhotso for the support throughout the project
- Timothy Hlongwane for the support
- Bokang Molatlhwa for the support
- Lungelo Ntamane for being there every step of the way
- Lesego Mogoboya for the support throughout the project
- Sharon Stewart for ensuring that I am up to date with my submissions
- My brother Simon for assisting me when I had laptop issues
- To the #100KidsToVarsity Executives, Directors, and members for pushing me to achieve more every single year

Achievements and awards

- **2018: Institute of Risk Management (IRMSA)**- Educational Risk Influencer of The Year Top 5 Finalist.
- **2019: GradStar**- Top 100 Finalist for the most employable university students of South Africa.
- **2020: Waterberg District Mayoral Awards Winner**- Community Builder of the year.
- **2020: Mzansi Youth Awards Nominee**- Best Male Academic Achiever, Community Builder of the year, and Businessman of the year.
- **2020: GradStar**- Top 100 Finalist Most employable University students of South Africa

Table of Contents

List of uncommon abbreviations

ADME- Absorption Distribution Metabolism, and Excretion

DMEM- Dulbecco Modified Eagle Medium

DMSO- Dimethyl sulfoxide

DPPH- 2, 2-diphenyl-1-picrylhydrazyl

FBS- Foetal Bovine Serum

GPx-Glutathione peroxidase

HMG-1- High Mobility Group 1 Protein

MEM- Modified Eagle Medium

MTT- (3-(4, 5-Dimethylthiazol-2-yl)-2, 5-diphenyltetrazolium bromide)

NAMI-A- ImH] [trans-RuCl4 (DMSO) (Im)]

NOS- Nitric Oxide Synthase

ROS- Reactive Oxygen Species

RPMI- Roswell Park Memorial Institute

SI- Selectivity Index

TRX- Thioredoxin

List of Figures

List of tables

CHAPTER 1: LITERATURE REVIEW

1.1 Introduction

Cancer is a genetic disorder characterized by an uncontrollable cell growth caused by a malfunction in the genes controlling the growth and division phases of the cell cycle (Plaks et al., 2015). Cancer can be hereditary or may develop due to DNA damage by cancer-causing agents known as carcinogens. These carcinogens include tobacco use, UV exposure, medical treatment, and drugs that suppresses the immune system which causes genetic changes to normal cells (Vineis et al., 2014). Proto-oncogenes (***Figure 1***), tumour-repressor genes and DNA-repair genes are affected by cancer-causing genetic changes (Plaks et al., 2015). The proteins encoded by these genes inhibit cell differentiation and halt cell death (Cantara et al., 2010). All these processes are important for normal human development and the maintenance of tissues and organs. These mutations often lead to increased oxidative stress, increased cell division, decreased cell differentiation, and inhibition of normal cell death (apoptosis) (Romeo et al., 2011).

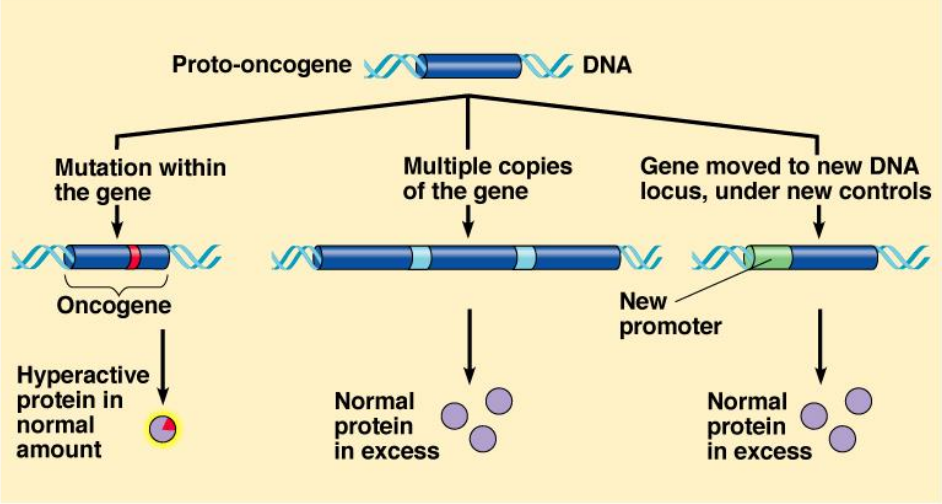

Figure 1: Oncogene development. *Processes that change proto-oncogenes to oncogenes (transformation) may include simple mutations of the proto-oncogene where the gene now makes hyperactive proteins with altered structure and function. From: Selfors et al., 2017*

This study investigated the effects of 12 novel complexes for the reduction of oxidative stress and the induction of apoptosis in cancerous cells. The three cancer cell types, which were studied, were HeLa, HepG2 and U937 cells; and the mammalian Vero cell line was used to determine the selectivity of each complex. The three different cancers associated with these cell lines are discussed in more detail below.

1.2 Cervical cancer

A virus called the Human Papillomavirus (HPV) (deMartel et al., 2015) causes cervical cancer. The virus spreads through sexual contact and with time may lead to cervical cancer (Wright et al., 2015). Females who are at higher risk of developing cervical cancer are smokers, individuals who have had many children, women who use birth control pills for a long time or have HIV infection (Arbyn et al., 2015). Health care providers can find abnormal cells through a Papanicolaou (Pap) test to examine cells from the cervix or by having an HPV test. Individuals can find and treat any problems before they turn into cancer when they undergo regular screenings (Koliopoulos et al., 2017). Treatment may include surgery where the tumour is surgically removed, radiation therapy, chemotherapy, or a combination of different treatments as seen when cancer patients undergo both chemotherapy and radiation therapy simultaneously. Metal complexes are currently being investigated for their ability to reduce cervical cancer progression (Gill and Vallis., 2019).

1.3 Leukaemia

Leukaemia is a cancer caused by the impairment of mutation of blood-forming tissues (Kipps et al., 2017). In people with leukaemia, the bone marrow produces abnormal white blood cells, which do not function properly (Neoh et al., 2015). DNA mutation causes acute myeloid leukaemia (AML) in the stem cells in the bone marrow. The mutation causes an overproduction of white blood cells. Treatment for leukaemia can be complex depending on the type of leukaemia and other factors. Treatment includes monitoring, chemotherapy, followed by radiation therapy and stem cell. Metal complexes are currently being investigated for their antitumor ability against chronic lymphocytic leukaemia cells (Silconi et al., 2015).

1.4 Liver cancer

Liver cancer (hepatocellular carcinoma) begins in the cells of the liver (Ryerson et al., 2016). Other types of liver cancer, such as intrahepatic cholangiocarcinoma (a type of cancer, which forms in the bile ducts) and hepatoblastoma (cancer occurring in infants and children) are much less common (Bergquist et al., 2015). Cancer that spreads to the liver is more common than cancer that begins in the liver cells. Liver cancer treatment is available which includes and not limited to surgery or chemotherapy. The use of metal complexes to treat liver cancer has also been investigated over the past

decade (Liu et al., 2015). Chemotherapy and the use of anticancer metal complexes to combat the progression of cancer will be discussed in more detail below.

1.5 Oxidative stress

Normally there is a strict balance between the cell's reactive oxygen species (ROS) and the production of antioxidant defences (Valco et al., 2006). Ros deregulate this balance or homeostasis ultimately leading to tumorigenesis (DeNicola et al., 2011). Ultraviolet (UV) exposures, and other carcinogens increase cancer ROS production leading to the inability of the cancer cells to undergo apoptosis (Prasad et al., 2017). Oxidative stress plays a significant role in in the development of various cancers such as liver cancer cervical cancer, leukaemia, and prostate cancer (Thanan et al., 2015). Nitric oxide (NO) is renowned for its role as a messenger or effector signalling molecule. This free radical is generated endogenously from the metabolism of L-arginine to L-citrulline through a complex reaction catalysed by various NADPH-dependent enzymes called nitric oxide synthase (NOS) (Wendehenne et al., 2004). Up-regulation of NOS and elevated NO activity is frequently detected in tumour microenvironments (Fukumuraet al., 2006). NO can be derived from tumour cells themselves and neighbouring cells (Chiribella., 2012). NO is lipophilic making it able to diffuse between cells to affect the tumour phenotypes of neighbouring cells (Postovit et al., 2005). It has been reported that NO at micromolar concentrations can promote cancer progression while a high NO concentration leads to the targeted decrease in cancer progression (Weiming et al., 2002).

1.6 Chemotherapy

The current cancer treatment methods as previously mentioned include chemotherapy, radiation, surgery, stem cell transplant, hormonal therapy, and immunotherapy. Chemotherapy mainly consists of the administration of a variety of drugs either orally, intramuscular, into the fluid that surrounds the spinal cord and brain, or intravenously (Reck et al., 2016). Chemotherapy is sometimes also combined with radiation therapy (Blanchard et al., 2015). Chemotherapy agents help increase the sensitivity to radiation (Karagianis et al., 2017). The administration of chemotherapy and radiation therapy at the same time offers the same benefits as sequential timing. Many anticancer drugs are designed to target DNA, and cisplatin is one most effective DNA-damaging agents (Jamieson and Lippard., 2006). Ever since the discovery of cisplatin by Rosenberg *et al* in 1965, a lot of research focused on this

platinum complex. Cisplatin is also used for the treatment of various cancers including advanced bladder cancer, metastatic ovarian cancer, metastatic testicular cancer, and testicular cancers (Theon et al., 1993). Its mode of action is relatively simple; Cisplatin kills cancer cells by intercalating itself within the DNA causing the normal cell repair mechanism to be nonfunction leading ultimately to cell death (De Luca et al., 2019). The cisplatin-DNA complex attracts the attention of HMG (high mobility group)-one and other DNA repair proteins, which become irreversibly bound (Zhu et al., 2016). The resulting distortion to the shape of the DNA prevents effective repair. The trans isomer of cisplatin is unable to form two intra-strand links and lacks antineoplastic activity and that is why cisplatin, instead of transplatin is used for cancer treatment (Petrovic et al., 2016). Although cisplatin has been shown to target DNA, other metal complexes have been investigated for their various cellular-level targets. These targets include DNA synthesis by antimetabolites, DNA transcription and duplication targets by intercalating agents, and mitosis by spindle poisons (Fritzs et al., 2006).

1.7 Cell death

Multicellular organisms contain a number of cells that are connected part of an organized family (Garcia-Belinchón et al., 2015). All normal cellular functions are terminated by cell death (Garcia-Belinchón et al., 2015). Non-programmed cell death could be due to injury (Green et al., 2015). Clean up of cell debris by phagocytes of the immune system is more difficult during necrosis, as the disorderly death does not send signals, which tell nearby phagocytes to engulf the dying cell (Prasad et al., 2017). The release of intracellular content after cellular membrane damage is the cause of inflammation in necrosis. Programmed cell death is called apoptosis, where the cell undergo suicide and lyse without damaging neighbouring cells. A variety of metal complexes are being investigated for their potential anticancer abilities, where the induction of apoptosis is one of the characteristics of anticancer metal complexes (Mitra et al., 2014). Metal complexes induce apoptosis by forming DNA crosslinks, which then form kinks in the DNA that are not repaired by the normal DNA repair mechanism. Alkylating agents like cisplatin causes DNA crosslinks that inhibit DNA replication and RNA transcription (Fu et al., 2012).

1.8 The apoptotic pathway

Apoptosis occurs via the intrinsic or the extrinsic pathways (**Figure 2**). Both pathways end at the execution phase (Beurel and Job., 2006). The intrinsic pathway is

modulated Bcl-2 and Bax molecules. Activation of Bax leads to the formation of Bax-Bax dimers. These dimers enhance the cell's susceptibility to apoptosis (Josefsson et al., 2014). The Bcl-2 family oversees the balance because it has both thee pro- and anti-apoptotic members (Josefsson et al., 2014). When a ligand binds to the external death receptors this triggers the extrinsic pathway (Fulda and Debatin., 2006). These receptors are members of the Tumour Necrosis Factor Receptor (TNFR) gene family, such as TNFR1 or FAS (Ji et al., 2019). This binding to the receptors leads to downstream caspase activation (Ji et al., 2019).

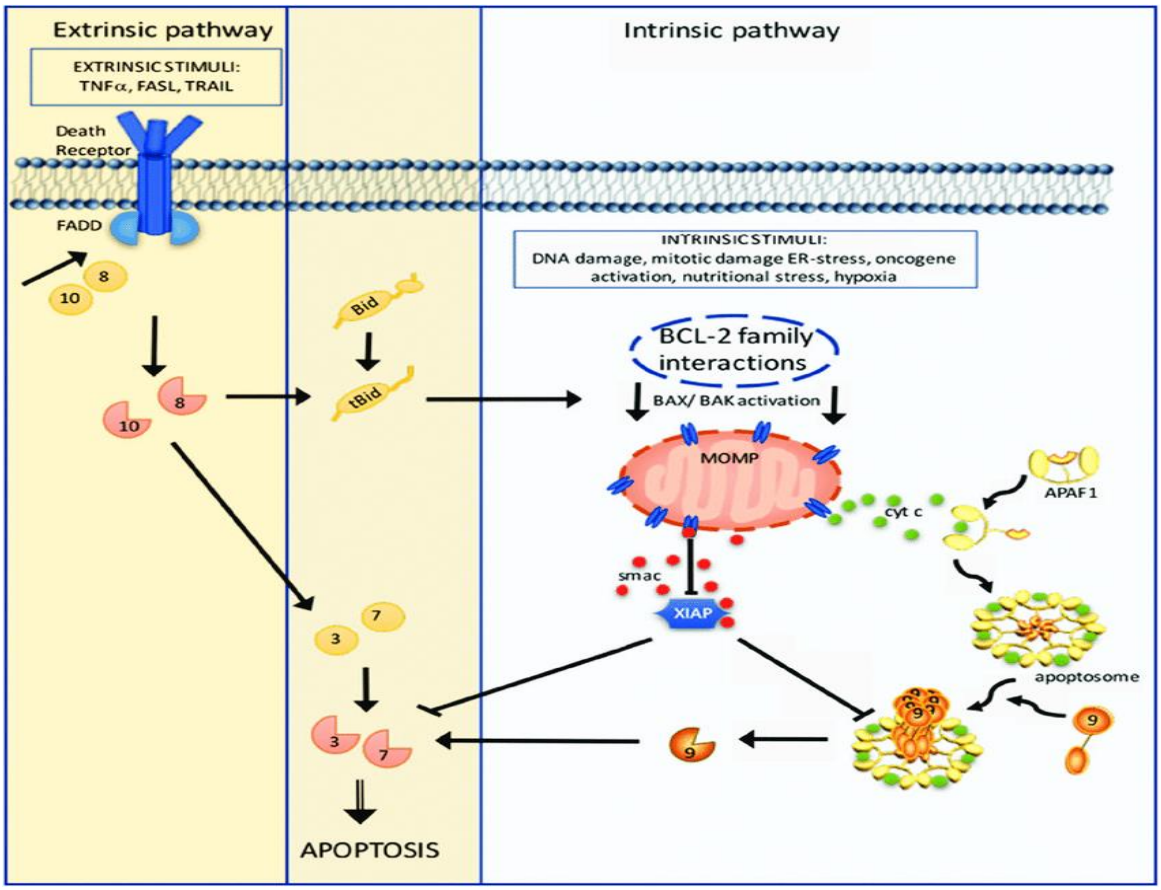

Figure 2: The extrinsic and intrinsic apoptotic pathways. *The extrinsic pathway is initiated by engagement of death receptors (DRs) via their respective ligands; tumour necrosis factor (TNF), FASL/CD95L, or TNF-related apoptosis-inducing ligand (TRAIL). Together with the adaptor Fas-associated death-domain (FADD) protein and the initiator procaspase-8 (or-10) they form the death-inducing signalling complex (DISC). This assembly enables the dimerization and autoactivation of the initiator caspases, which in turn cleave and activate the executioner caspase-3 and-7, ultimately leading to apoptosis unless they are inhibited by X-linked inhibitor of apoptosis protein (XIAP). The intrinsic pathway can be engaged by diverse intracellular stresses that modulate BCL-2 family protein interactions that control the activation of the BCL-2 effector proteins BAX and BAK. Once activated, BAX and BAK cause mitochondrial outer membrane permeabilization (MOMP), leading to the release of proapoptotic intermembrane space (IMS) proteins. Cytochrome c (Cyt c) engages Apoptotic protease activating factor 1 (APAF1) and induces its oligomerization, leading to apoptosome formation that recruits and activates the initiator*

procaspase-9. Active caspase-9 cleaves and activates the executioner caspase-3 and-7. Simultaneously with Cyt c, Smac is released from the IMS and inhibits XIAP. The extrinsic and intrinsic pathways are linked; caspase-8 can cleave the BH3-only protein BH3-interacting domain death agonist (Bid), leading to its active, truncated form tBid, which in turn activates BAX/BAK. Numbers in circles indicate the respective pro-and active caspase; interrupted circles represent active caspases (Buerel and Jobe., 2006).

The metal complexes currently in clinical usage have been shown to induce apoptosis. These are discussed further in the paragraph below.

1.9 Metal Complexes as potential anti-cancer agents

Metal complexes have been used since 3500BC, where gold has been reported to reduce inflammation (Bergamo et al., 2015). Iron has been used for the treatment of anaemia while sodium vanadate has also been used in the 20th century for the treatment of rheumatoid arthritis (Bergamo et al., 2015). Gold metal complexes show great anti-tumour activity when compared to cisplatin where studies have been conducted showing the anticancer properties of gold-based metal complexes. Ndagi et al., (2017) reported a series of Au^{III} metal complexes with N-heterocyclic carbine ligands, which can be used as both thiol fluorescent probes and as anticancer agents. Metal complexes of platinum, ruthenium, titanium, and gold are the most studied and all these metal complexes have been reported to have anti-tumour activity (Jungwirth et al., 2011). Platinum complexes (***Figure 3***) as aforementioned have DNA-binding activity, while gold and titanium complexes have been reported to have antitumor activity when tested on cervical and human colon cancers (Wenzel et al., 2011). All these complexes after administration are metabolized into a pharmacologically active drug, where this activity improves the absorption, distribution, metabolism, and excretion (ADME) of the complexes (Graf et al., 2012). FDA-approved metal-based anticancer drugs currently in clinical usage are cisplatin, carboplatin, and oxaliplatin (Picone et al., 2017). Nedaplatin, lobaplatin, and heptaplatin are approved for clinical usage in Japan, China, and Korea respectively. When tested *in vitro*, most of the complexes demonstrated the highest cytotoxicity. When evaluated *in vivo* using nude mice bearing HeLa xenografts, the complexes showed a significant reduction in tumour volume. Islam et al., 2017 showed that Au^{III} dithiocarbamate complexes could be promising anticancer agents based on their ability to target deubiquitinases (proteases that cleave ubiquitin from proteins and other molecules) in breast carcinoma MCF7 cells. This gold complex is more cytotoxic than cisplatin with a CC_{50}

of 1.04 µM and induced cell cycle arrest in S-phase and G2-phase. Hargrove et al., 2015 reported Au^{I}/Au^{II} complexes with imidazole derivatives, which were evaluated against ovarian and breast carcinoma cell lines.

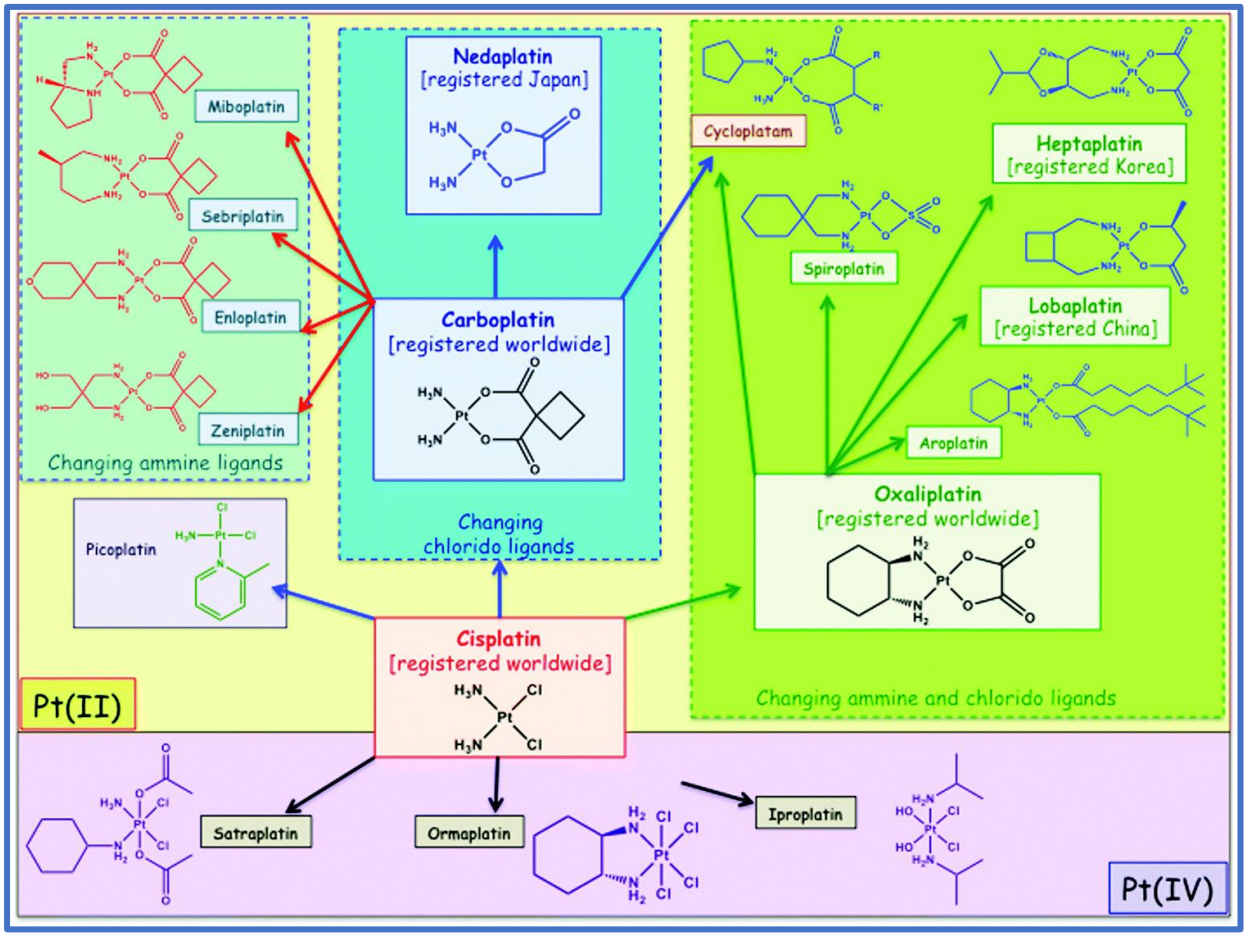

Figure 3: Anticancer platinum-based metal complexes. *These are some of the cisplatin analogues to date. They were created to reduce the dire side side-effects associated with cisplatin chemotherapy treatment. From: Picone et al., 2017*

1.10 Gold-based metal complexes

Auranofin is an example of a gold-based metal drug currently available commercially. The World Health Organization (WHO) classifies auranofin as an anti-rheumatic agent (Fiskus et al., 2014) classifies this drug. The complex is used in the treatment of and the improvement of symptoms of arthritis, which is an inflammation of one or more joints (Harbut et al., 2015). Unlike cisplatin, the mechanism of action of Auranofin includes the inhibition of redox enzymes glutathione peroxidase (GPX) (***Figure 4***) and thioredoxin (TrxR). Auranofin has a thiol ligand that has a high affinity for thiol and selenol groups, which are physiological free radical scavengers. The side effects

include itching or skin rash, severe or ongoing diarrhoea, vomiting and stomach cramps.

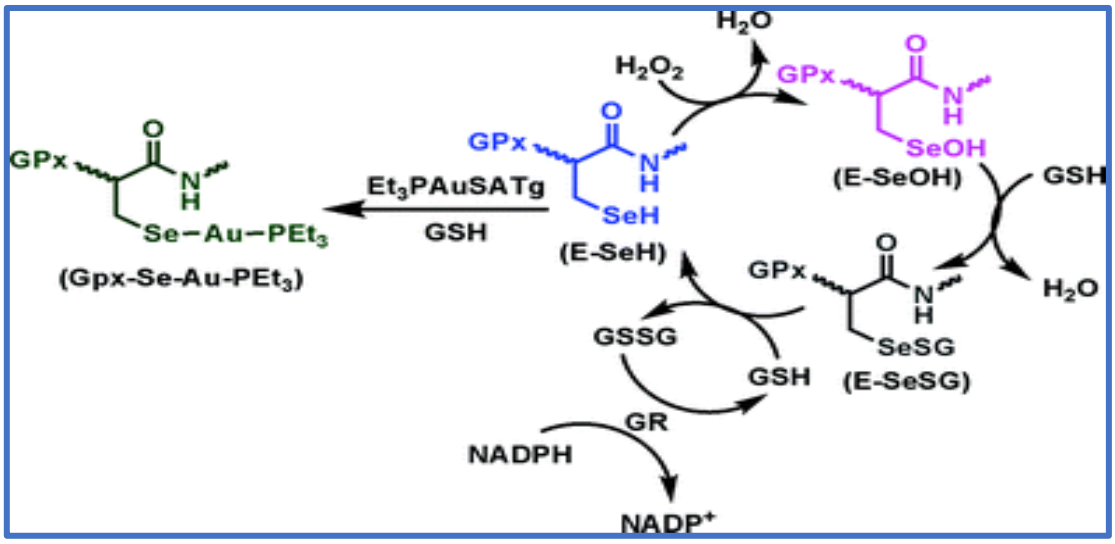

Figure 4: Auranofin mechanism of action. *Inhibition of the antioxidant activity of (GPx) by Auranofin. The reaction of selenol with Auranofin produces the corresponding stable form of the gold-selenolate (GPx-Se-Au-PEt3) complex intracellular. From: Harbut et al., 2015*

Che et al., 2010 reported that the novel gold (III) exhibited strong cytotoxicity in some tumour cell lines. Gold 1a exhibited cytotoxic effects *in vitro* to human colon cancer, and the concentration of drug required to inhibit cell growth by 50% (CC_{50}) values ranged from 0.2 µM to 3.4 µM, which represented 8.7-fold to 20.8-fold greater potency than that of cisplatin. Gold 1a significantly induced apoptosis and cell cycle arrest and cleaved the tumour promoters; caspase 3, caspase seven, and poly (ADP-ribose) polymerase; released cytochrome C, and up-regulated the tumour inhibitors p53, p21, p27, and Bax. *In vivo*, intraperitoneal injection of gold 1a at doses of 1.5 mg/Kg and 3.0 mg/Kg significantly inhibited tumour cell proliferation, induced apoptosis, and suppressed colon cancer tumour growth. An acute toxicology study indicated that gold 1a at effective antitumor concentrations did not cause any toxic side effects in mice.

1.11 Ruthenium complexes

Ruthenium has two main oxidation states, Ru (II) and Ru (III) (Dharmaraj et al., 2001). Many metal complexes contain exchangeable ligands and require activation by the tumour microenvironment. The antitumor properties of the Ru (III) complexes occur when they are reduced to their corresponding Ru (II) counterparts *in vivo* (Noyori et al., 1997). Under cancerous conditions such as low oxygen concentration, acidic pH

and high levels of glutathione, the Ru (II/III) redox potential can be altered, and thus Ru (III) complexes can be reduced to Ru(II) complexes (Adam et al., 2016). NAMI-A, [ImH][trans-RuCl4(DMSO)(Im)] (Im = imidazole, DMSO = dimethyl sulfoxide; has low potency in terms of direct cytotoxicity towards cancer cells *in vitro*; however, *in vivo*, it has significant efficacy in inhibiting tumour metastasis (the development of secondary malignant growths at a distance from a primary site of cancer) (Leijen et al, 2015). Data has shown that NAMI-A is capable of binding to DNA and RNA (Agonigi et al., 2015). It can bind to the histidine residues of serum albumin under physiological conditions indicating poor efficacy (Agonigi et al., 2015). However, the low therapeutic efficiency, progression of the disease in the clinical studies (phase I) and partial response (phase I/II) limited further clinical use of NAMI-A and failed the clinical investigations (Bergamo et al., 2017).Subsequently, KP1019 [trans-tetrachlorobis-(1H-indazole) ruthenate (III)] designed by the Keppler group entered clinical trials but its low solubility limits its further development. A more soluble sodium salt, KP1339 (trans-(tetrachlorobis (1H-indazole) ruthenate (III)), is currently undergoing clinical trials (Chang et al., 2016).

The current cancer treatment using cisplatin has dire side effects. Therefore, in this project novel, gold and ruthenium complexes were investigated for potential anti-cancer activity.

1.12 The drug discovery pipeline

Drug discovery consists of multiple steps and the process can go on for several decades (Van Dam et al., 2011). Phase 1: Target identification. This is the first phase in the long discovery pipeline (Wishart., 2007). Phase 2: Lead discovery. This is where chemical compounds are synthesized to interact with specific targets (Duffy et al., 2012). Phase 3: Medicinal chemistry: this is where a library of compounds along with their analogues are developed. In this phase the structure-activity relationship (SAR) is evaluated as well as *in silico* studies (Lücking et al., 2013). Phase 4: In vitro studies. This is the lead optimization stage that occurs *in vitro* (Hochman et al., 2002). Phase 5: In vivo studies. In vivo studies occur once the leads have been optimised (van der Greef and McBurney., 2005). Phase 6: Clinical Trials. Clinical trials in humans can be initiated once the leads have passed all the above-mentioned trials. (Mishra and Tiwari., 2011). Phase 7: FDA approval and commercialization. Once the lead compound passed clinical trials and have received adequate review the compound

can now be used clinically world-wide. (Patridge et al., 2016). This study falls in the fourth phase of the drug discover pipeline (Chen et al., 2011). Several in silico drug discover tools are available. Some of these tools include the protein docking algorithm EADock, Avogadro, Discovery Studio, Materials Studio, and Molinspiration (DeLano., 2005). Molinspiration was chosen for this study because it is a freeware and it gives accurate results. Molinspiration calculations are based on Lipinski's rule of 5 (Patela et al., 2016). The rule describes molecular properties important for a drug's pharmacokinetics in the human body, including their absorption, distribution, metabolism, and excretion ("ADME") (Lipinski., 2004). Lipinski's rule states that for drugs or drug candidates to be orally active they must not be larger than 500 daltons, they must not have more than 5 hydrogen donors, they must not have more than 10 hydrogen acceptors, the partition coefficient (log P) must not be more than 5, they must not have more than 10 rotatable bonds, and the polar surface area must not be greater than 140 Å. These are the indicators that the complexes of the study were tested and evaluated on (Nogara et al., 2015).

The following research questions were generated for the study:

- Can the metal complexes inhibit the growth of HeLa (cervical cancer), U937 (Leukaemia), and HepG2 (liver cancer) cells?
- What are the CC_{50} values of these complexes on the tested cancer cell lines?
- Are the complexes selective for cancerous cells?
- Do the complexes have antioxidant activity?
- Are the complexes able to induce apoptosis?
- What is the overall drug-likeness of the complexes?

1.13 Hypothesis

The hypothesis of the study was:

H_1: Gold and ruthenium complexes should have *in vitro* anti-cancer activity with significant antioxidant and apoptosis-induction activity.

H_0: Gold and ruthenium complexes should not have *in vitro* anti-cancer activity with significant antioxidant and apoptosis-induction activity.

1.14 Aims and objectives

The project aimed to determine the anticancer activity of novel ruthenium and gold-based complexes on HeLa, U937, and HepG2 cell lines.

The objectives were therefore to:

- Determine the 50% cytotoxic concentration (CC_{50}) of the complexes using the MTT tetrazolium dye
- Determine the antioxidant activity of the metal complexes using the DPPH and NO assays
- Assess drug-induced apoptosis through flow cytometry
- Determine the drug-likeness of the complexes

CHAPTER 2: MATERIALS & METHODS

All reagents used were of analytical and cell-culture grade. Please see **Appendix I** for the list of all reagents and company information. All used formulae are presented in **Appendix II**.

2.1 Complex information

The metal complexes were synthesized at the University of Johannesburg by Dr Christian Odokoh (gold metal complexes) and Dr Gershon Amenuvor (ruthenium complexes) under the supervision of Prof James Darkwa and Dr Banothile Makhubela. Some synthesis information is provided below.

2.1.1 Synthesis of [2-(diphenylphosphino) ethyl] aminegold (I) chloride (AE215)

The title complex **AE215** was prepared according to a literature procedure from [Au (tht) Cl], which was obtained by reacting H [$AuCl_4$].3H_2O with tetrahydrothiophene (tht) in ethanol. A dichloromethane solution of [Au (tht) Cl] (0.26 g, 0.87 mmol) was added to a solution of 2-(diphenylphosphino) ethanamine (**L1**) (0.20 g, 0.87 mmol) in dichloromethane (10 mL) and stirred for 3 hours. The solvent was reduced to half and hexane was added until white precipitate formed. The white solid obtained was filtered and dried *in vacuo.*

2.1.2 Synthesis of [3-(diphenylphosphino) propyl] aminegold (I) chloride (AE207)

Complex **AE207** was prepared using similar method discussed for complex **AE215** with the following reagents: three-(diphenylphosphino) propanamine (0.44 g, 1.8 mmol) and Au (tht) Cl (0.58 g, 1.8 mmol).

2.1.3 Synthesis of [2-gluconamidoethane-2-(diphenylphosphino) ethyl] amine gold (G3)

The synthesis of **G3** was performed according to the literature method with slight modifications. D-(+)-gluconic acid δ-lactone (0.1 g, 0.56 mmol) was dissolved in methanol (30 mL) at 50 °C. After allowing the solution to cool down to room temperature, [2-(diphenylphosphino) ethyl] aminegold (I) chloride (**AE215**) (0.26 g, 0.56 mmol) was added. The mixture was then stirred overnight at room temperature and the solution reduced to half after which hexane was added until white precipitate formed. The white precipitate so obtained was filtered and washed successively with hexane (3 x 10 mL) to afford a white solid of **G3.**

2.1.4 Synthesis of [three-gluconamidoethane-3-(diphenylphosphino) propyl] amine gold (I) (G4).

The synthesis of **G4** was performed according to the method described for **G3** with the following reagents: D-(+)-gluconic acid δ-lactone (0.06 g, 0.34 mmol) and [2-(diphenylphosphino) ethyl] aminegold (I) chloride (**AE215**) (0.15 g, 0.34 mmol).

2.1.5 Synthesis of [acetylated-2-gluconamidoethyl (diphenylphosphino)] gold (I) complex (G5)

To a solution of **G3** (0.12 g, 0.18 mmol) and acetic anhydride (0.10 mL, 1.10 mmol) (1:1 ratio to hydroxyl group) in pyridine (2 mL), was added catalytic amount of dimethylaminopyridine (DMAP). The solution was stirred at room temperature for 18 h. The mixture was then diluted with dichloromethane (20 mL) and washed with 1M $HCl_{(aq)}$ solution (5 x 30 mL). The organic layer was dried using anhydrous $MgSO_4$ after which solvent was pumped off using rotary evaporator to give white solid.

2.1.6 Synthesis of [acetylated-3-gluconamidopropyl (diphenylphosphino)] gold (I) complex (G6)

To a solution of **G4** (0.10 g, 0.15 mmol) and acetic anhydride (0.08 mL, 0.75 mmol) (1:1 ratio to hydroxyl group) in pyridine (2 mL), was added catalytic amount of dimethylaminopyridine (DMAP). The solution was stirred at room temperature for 18 h. The mixture was then diluted with dichloromethane (20 mL) and washed with 1M $HCl_{(aq)}$ solution (5 x 30 mL). The organic layer was dried using anhydrous $MgSO_4$ after which solvent was pumped off using rotary evaporator to give white solid.

2.1.7 Synthesis of [2-(diphenylphosphino) ethyl] amine acetyl-2-gluconamidoethane thiolate gold (I) complex (G7)

Complex **AE215** (0.2 g, 0.43 mmol) and acetylated 2-gluconamidoethane thiol (0.2 g, 0.43 mmol 1 equiv.) were dissolved in 20 mL dichloromethane and 0.06 mL of triethylamine was added. The reaction mixture was allowed to stir overnight at ambient temperature. A white precipitate formed upon addition of hexane, which was filtered by suction filtration and dried under *vacuo* to afford white solid.

2.1.8 Synthesis of [3-(diphenylphosphino) propyl] amine acetyl-2-gluconamidoethane thiolate gold (I) complex (G8)

Complex **AE207** (0.20 g, 0.42 mmol) and acetylated 2-gluconamidoethane thiol (0.20 g, 0.43 mmol 1 equiv.) were dissolved in 20 mL dichloromethane and 0.06 mL of triethylamine was added. The reaction mixture was allowed to stir for overnight at

ambient temperature. A white precipitate formed upon addition of hexane, which was filtered by suction filtration and dried under *vacuo* to afford white solid.

2.1.9 Synthesis of R1

To a toluene solution (30 mL) of 2.53 mmol (0.90 g) of dimethyl 4,4'-((ethane-1,2-diylbis(azanediyl)) bis(methylene)) dibenzoate stirring at 0-5 ºC under argon atmosphere, was added triethylamine (20.00 mmol, 2.80 mL). The mixture was stirred for 10 minutes followed by addition of chlorodiphenylphosphine, (5.03 mmol, 0.38 mL) in a dropwise manner. The mixture was stirred at room temperature for 1 h and the precipitates obtained were filtered off using a filter paper and washed with 20 mL of toluene. The precipitates were dissolved in 50 mL of chloroform and washed successively with water (3x50 mL) to remove the triethylammonium chloride. The organic phase was dried over anhydrous $MgSO_4$ and filtered through a filter paper. The pure product was obtained as white solids in 55% yield upon evaporation of the solvent followed by drying.

2.1.10 Synthesis of R2

A dichloromethane solution (15 mL) of [Ru(p-cymene) $Cl_2]_2$ (0.0413 mg, 0.067 mmol) was mixed with a 15 mL dichloromethane solution of ligand **R1** (0.098 mg, 0.135 mmol). The solution was stirred at room temperature for 2 h. The resulting solution was concentrated, and the products precipitated with hexane and filtered off as a reddish brown solid.

2.1.11 Synthesis of R3

A dichloromethane solution (15 mL) of [Ru(p-cymene) $Cl_2]_2$ (0.084 g, 1.380 mmol) was mixed with ligand **R1** (0.100 g, 0.140 mmol) dissolved in 15 mL of dichloromethane. The solution mixture was stirred at room temperature for 2 h. The resulting solution was concentrated, and the products precipitated with hexane and filtered off as a reddish brown solid.

2.1.12 Synthesis of R4

A dichloromethane solution (15 mL) of [Ru(p-cymene) $Cl_2]_2$ (0.0413 mg, 0.067 mmol) was mixed with a 15 mL dichloromethane solution of ligand R1 (0.098 mg, 0.135 mmol). The solution was stirred at room temperature for 2 h. The resulting solution was concentrated, and the products precipitated with hexane and filtered off as a reddish brown solid.

Table 1 indicates all gold complexes that were synthesized and tested in this study whereas the ruthenium complexes are shown in **Table 2**

***Table 1**: The molecular structures of the gold metal complexes tested, where cisplatin was used as a control.*

Code	Molecular weight	Structure	Novelty
AE215	461.67	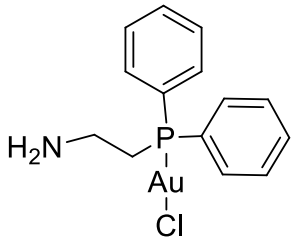	Known (Khan et al., 1993)
G3	639.81	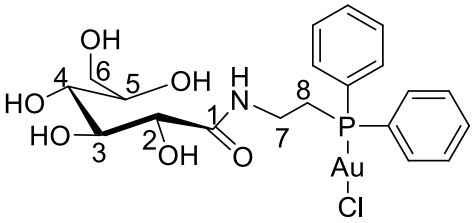	Novel
G5	850.00	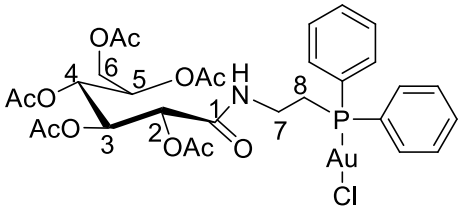	Novel
G7	890.68	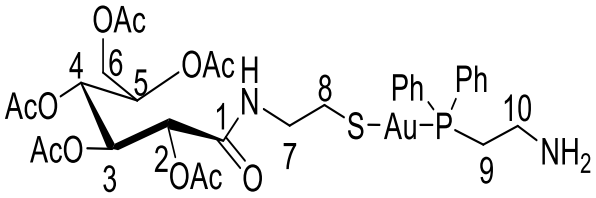	Novel
AE207	475.70	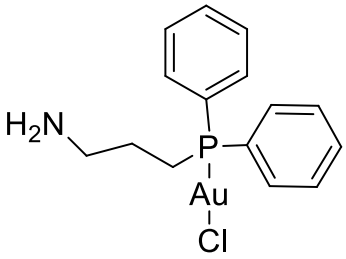	Novel

G4	653.84	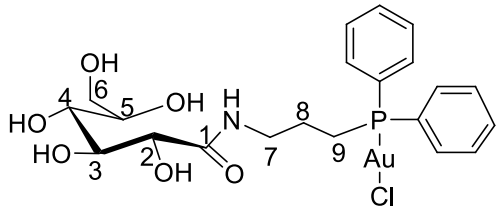	Novel
G6	864.02	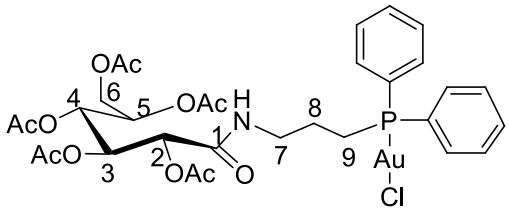	Novel
G8	904.71	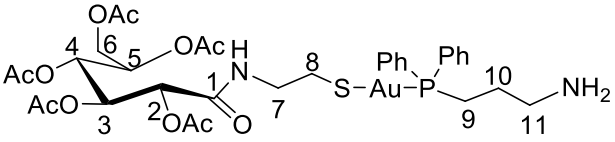	Novel
Cisplatin	300.05	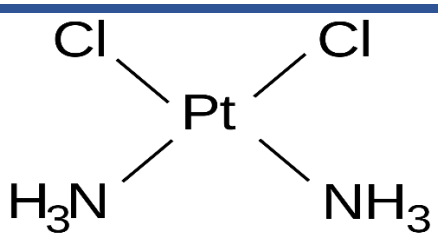	Control
Auranofin	679.49	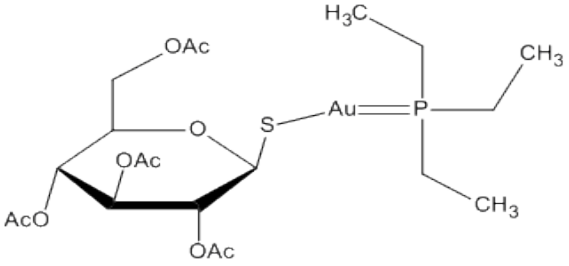	Control

***Table 2: Ruthenium metal complexes**. R1 is a ligand while complexes R2, R3, and R4 are the derivatives.*

Code	Molecular weight	Structure	Novelty
R1 (ligand for R2 R4, and R3)	724.76 g/mol	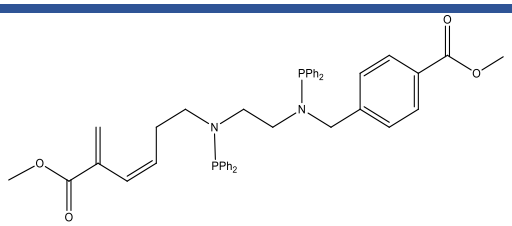	Novel
R2	1030.95 g/mol	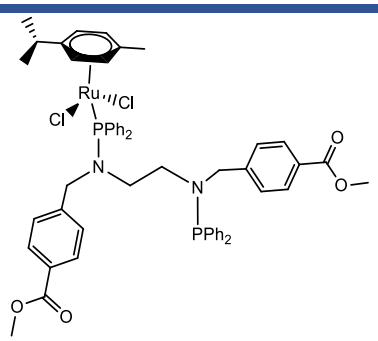	Novel
R3	1352.18 g/mol	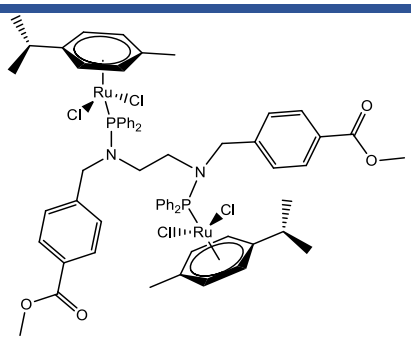	Novel
R4	1353.19 g/mol	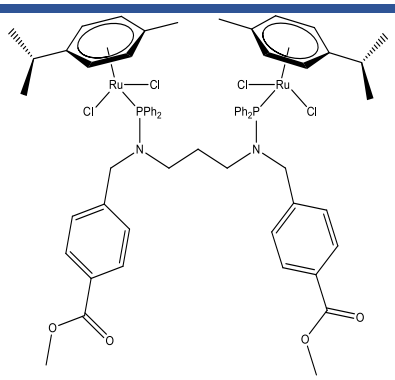	Novel

2.2 Cell culture and propagation

Three cancer cell lines were chosen for the project based on the type of cancers which are cause the most cancer-related deaths in southern Africa and the cell lines were HeLa, HepG2, an U937 cell lines. These are cell lines derived from the three types of cancers, which are closely related to HIV infection (Coghill et al., 2015). HepG2 cells are an immortalized human liver cancer cell line. This is an adherent cell line most commonly used to evaluate drug metabolism and hepatotoxicity (Huang et al., 2017). The HeLa cell line is an immortalized cell line derived from a cervical cancer patient. Over the years, these cells have furthered the understanding of not only cancer but cell morphology in general (Duan et al., 2016). These cells are widely used to grow viruses and for the evaluation of new anticancer medicines (Li et al., 2015). The human monoblastic leukaemia cell line, U937 has been the subject of studies of hemopoietic cell differentiation *in vitro.* This is a nonadherent acute leukaemia cell line (Bidovec et al., 2017). Derived from the kidney of an African green monkey in the 1960s, Vero cells are one of the most common mammalian cell lines used in research (Zeng et al., 2015). These Vero adherent cell lines were used as a control cell line in this study (Menezo et al., 1989).

2.2.1 Thawing, culturing and passaging of Cell lines

The HepG2 and Vero cell lines were thawed in Dulbecco Modified Eagle Medium (DMEM) supplemented with 5% HEPES buffer (v/v), 1.1 % sodium pyruvate (v/v), 1% Gentamicin (v/v) and 20 % foetal bovine serum (v/v) (FBS) and incubated overnight (37 °C; 5% CO_2, 95% humidity) in a 75 cm^3 aerated culture flask. The next day the spent media was removed and DMEM media supplemented with 10% FBS (v/v) was added (15 mL). The cells were incubated for 2-4 days and upon reaching 80% confluence, and they were trypsinized and detached from the bottom of the flask. The media was discarded and the cells were washed with pre-warmed 1% PBS (v/v) to remove residual media. Three millilitres of Trypsin-EDTA (Sigma-Aldrich, USA) was then added to the flask and left for 30 seconds at room temperature. After that, the trypsin was removed and the flask was incubated for 3 minutes (37 °C; 5% CO_2, 95% humidity). The cells were resuspended using fresh media and were counted using a haemocytometer and re-suspended at $1x10^5$ cell/mL. This method was only used for HepG2 and Vero cells, while Modified Eagle Medium (MEM) supplemented with 20%

FBS and 5% antibiotic/antimitotic was used for HeLa cells and Roswell Park Memorial Institute medium (RPMI) supplemented with 10% FBS (v/v) was added (15 mL) was used for U937cells. The U937 cells were suspension cells, passaging did not require the trypsinization step.

2.2.2 Effects of metal complexes on cell growth using the MTT assay

MTT assay is a colourimetric dye that is used for assessing metabolic activity and cell viability. The dye is light sensitive; therefore, all tests using MTT are conducted in the absence of light. MTT is based on the ability of nicotinamide adenine dinucleotide phosphate (NADPH)-dependent cellular oxidoreductase enzymes to reduce the tetrazolium dye MTT to its insoluble formazan, which has a purple color (Gerlier et al., 1986). MTT forms solid crystals when it reacts with the enzyme and the crystals are solubilized by acid and an absorbance of 550 nm with a reference of 690 nm was used in this assay.

Method: A volume of 100 µL media (supplemented with 10% FBS) was added to a 96-well plate where a dilution series of the complexes was performed to get complex concentrations of 0.78- 50 µM. A cell concentration of 1×10^5cells/mL was used per final volume of 200 µL in each well. The cells were then incubated for 72 hours (37 °C; 5% CO_2, 95% humidity) after that the residual media was discarded and 100 µL of MTT solution (5mg/mL) was added to each well. The cells were then incubated for a further 24 hours (37 °C; 5% CO_2, 95% humidity). After 24 hours all produced formazan crystals were solubilized with 100 µL Solubilisation buffer (1mL 1M HCl: 9 mL Isopropanol) and the absorbance of the samples was measured at 550 nm with a reference at 690 nm. A background control (media only), as well as untreated controls (cells only), were included in each experiment. Cisplatin was used as the standard cytotoxic control.

2.3 Determination of antioxidant activity using the DPPH assay.

This assay is based on the theory that a hydrogen donor is an antioxidant and it measures complexes that are radical scavengers of active oxygen species (Zhang et al., 2016). The complex 2, 2-diphenyl-1-picrylhydrazyl (DPPH) is one of the few stable and commercially available organic nitrogen radicals and the antioxidant effect of the free radical scavenger is proportional to the disappearance of DPPH in test samples. Monitoring DPPH with a UV spectrometer has become the most commonly used

method because of its simplicity and accuracy. This reaction from purple to yellow is stoichiometric concerning the number of hydrogen atoms absorbed. Therefore, the antioxidant effect can be easily evaluated by following the decrease in UV absorption at 550 nm. Vitamin C was used as the positive control.

Method: The complexes which were cytotoxic towards the cancerous cell lines and not cytotoxic towards the non-cancerous cell line were investigated for potential radical activity using DPPH. The assay was performed as described by Le Roux et al., 2011 and complex concentrations ranging from 1.6-100 µM were investigated. These were prepared with absolute ethanol in a 96-well microtiter plate (50 µL/well) and DPPH (0, 1 mM, 50 µL) was pipetted to each well. The plates were incubated in the dark for 30 minutes to allow scavenging; the absorbance was read using a 96-well microplate reader at 550 nm.

2.4 Determination of antioxidant activity using the NO assay.

Nitrite is a central homeostatic molecule in NO biology and serves as an important signalling molecule in its own right. Nitrite and nitrate in blood have been widely used as an index of endothelial NO synthase activity as routine indirect measures of NO levels. Excessive NO can also cause disease, It may damage brain cells leading to neurodegenerative diseases like Parkinson disease, Alzheimer disease, Huntington disease and amyotrophic lateral sclerosis. Metal containing proteins can catalyse the oxidation of NO to nitrite. The recent discoveries that nitrite can be reduced back to NO under appropriate physiological conditions and nitrite itself can directly nitrosate thiol to form S-nitrosothiols (RSNOs), has caused intense interest in this molecule. The concentration of nitrate produced depends mostly on the specific tissue culture media and biological fluids used (Murphy et al., 1994). The reaction takes place in a microtiter plate (Murphy et al., 1994).

Method: The active complexes (CC_{50}<10 µM; SI>1) were further assessed for their effects on NO levels of HeLa, HepG2 and U937 cells. The complexes which were cytotoxic towards the cancerous cell lines and not cytotoxic towards the non-cancerous cell line were tested at CC_{50} and $2XCC_{50}$ were the dose-response of the complexes was evaluated. Cells were cultured in a 96-well plate. Untreated cells were used as controls. The nitrate standard (0,1M) was diluted to 100 µM and a serial dilution was made. The cancerous cells were treated with the complexes to inhibit NO

production (for 72 hours). The plate containing cells was centrifuged. The supernatants were collected, and a volume of 50 µL of each treatment was transferred to a new 96-well plate. A volume of 50-µL sulphanilamide solution (1% in 5% phosphoric acid) was added to each sample including the controls and mixed well. The mixture was incubated at room temperature for 10 minutes in the dark. N-1-naphtylethylenediamene dihydrochloride solution (50 µL) was added to all samples and mixed well. The mixture was incubated in the dark at room temperature for 10 minutes and the absorbance was read using a microplate reader at 550 nm.

2.5 Apoptosis induction

Rationale: A common feature of apoptosis is the transfer of phosphatidylserine (PS), which ordinarily reside on the cytoplasmic surface of the membranes, to the cell surface. The PS that is externalized not only contributes to the recognition and subsequent removal of apoptotic bodies by phagocytes but also provides a binding site for the anionic lipid-binding protein Annexin V, which is widely used to detect apoptotic cells. In addition to its use in laboratory studies *in vitro*, Annexin V binding is being explored as a potential early marker of treatment efficacy in cancer patients.

Method: Cells were treated in a 24-well microtiter plate and treated with the active metal complexes at CC_{50} and $2xCC_{50}$ for 72 hours (37°C; 5% CO_2). Post-incubation 1 mL 1XPBS was added to the cells to wash off any residual media. A volume of 50 µL trypsin was added to each well to help the cells detach. After 10 seconds, trypsin was removed from the wells and a volume of 500 µL culture media was pipetted into each well. A volume of 500 µL of cells was added to tubes flow tubes (BD Biosciences; USA) after the incubation and was centrifuged (250×g; 5 minutes). The supernatants were discarded and a volume of 200 µL binding buffer was pipetted into each tube. FITC-Annexin V and Propidium iodide were added to each tube. The controls used were unstained cells, cells stained with FITC-Annexin V only cells stained with Propidium iodide (BD Biosciences; USA), and cells stained with both FITC-Annexin V and propidium iodide. The cells were then vortexed and incubated in the dark for 15 minutes. A volume of 200 µL binding buffer was then pipetted into each tube. Flow cytometry for each sample was performed using the BD Accuri G6.

2.6 *In-silico* ADME studies

An *in-silico* ADME computational study of the synthesized compounds was performed by determination of Lipinski's parameters. Lipinski rule of 5 helps in distinguishing

between drug-like and non-drug like molecules. It predicts a high probability of success or failure due to drug-likeness for molecules complying with 2 or more of the following rules. Calculations were performed using “Molinspiration online property calculation toolkit” (http://www.molinspiration.com). The values of miLogP, as (octanol/water partition coefficient) and TPSA of the investigated cephalosporins, were determined using the method developed by Molinspiration. Drug-likeness scores were calculated to represent the number of fragments based on contributions and correction factors.

2.7 Data Analysis

The percentage viability calculations were performed using Microsoft Excel 365 (2017). GraphPad Prism version 5.00 was used to determine complex CC_{50}. A Student’s t-test for unpaired observations was conducted using Microsoft Excel 365 This statistic method helps to compare the means of two independent sets of data. A $p < 0.05$ was considered significant. All data are presented as mean ± SEM where $n = 4$.

CHAPTER 3: RESULTS

3.1 Complex Cytotoxicity

The first step taken when testing our hypothesis was to determine the CC_{50} of the metal complexes on HeLa, HepG2, and U937 cells. The MTT assay was used for this test. The results obtained in ***Table 3*** and ***Figure 5*** showed that after 72 hours of treatment all of the complexes had CC_{50}< 25 µM. From these results, active complexes that had CC_{50}<10 µM across all cell lines were selected. Nine of the tested complexes were actively inhibiting HeLa cell progression as their CC_{50} were below 10 µM. Only complexes **G4**, **G6**, **G8**, and Cisplatin had CC_{50} of above 10 µM. The results obtained on HepG2 cells showed that 11 of the tested complexes were actively inhibiting cell progression with CC_{50} values being below 10 µM in this cell line. Only complex **G6** had a CC_{50} of above 10 µM showing that this complex was the least cytotoxic to this cell line with a CC_{50} of 12 µM. Finally, the cytotoxicity of the complexes was tested on U937 cells and it was seen that complexes **G5**, **G4**, **G6** and **R1** were the least cytotoxic with CC_{50} values of above the 10 µM cut-off concentration. A comparison between the parent complexes to their derivatives was made and it was seen that complex **G3** was the most cytotoxic compared to its parent **AE215**. The parent complex **AE207** was more cytotoxic than any of its three derivatives **G4**, **G6**, and **G8**. Complex **R3** was the most cytotoxic compared to the derivative **R1**.

The ruthenium complexes were more cytotoxic than the gold complexes when tested on all three cell lines. These complexes were even more cytotoxic than cisplatin.

Table 3: The complex CC_{50}. *The table below shows the CC50 values obtained after 72 hours of treatment on HeLa, HepG2, and U937 cells.*

Complex	HeLa CC_{50}	HepG2 CC_{50}	U937 CC_{50}
AE215	7.53±1.32	10.03±1.01	7.02±2.30
G3	4.64±1.11	7.25±0.35	5.03±1.86
G5	6.84±0.12	7.29±1.32	5.03±4.32
G7	5.28±1.32	8.66±1.82	8.53±1.89
AE207	6.12±2.36	6.02±2.36	4.24±0.32
G4	20.24±0.37	7.24±1.72	8.63±1.72
G6	10.01±1.62	14.25±1.38	13.24±1.30
G8	13.24±3.39	9.72±2.52	9.84±1.11
R1	2.63±1.24	6.01±1.33	11.24±1.42
R2	1.34±2.32	2.01±1.14	5.23±1.67
R3	6.01±0.12	1.01±0.62	4.48±1.72
R4	6.32±1.30	3.23±1.67	8.63±0.58
CIS	10.02±1.02	6.24±2.58	5.01±0.31
AUR	2.12±0.13	1.02±0.42	3.24±1.11

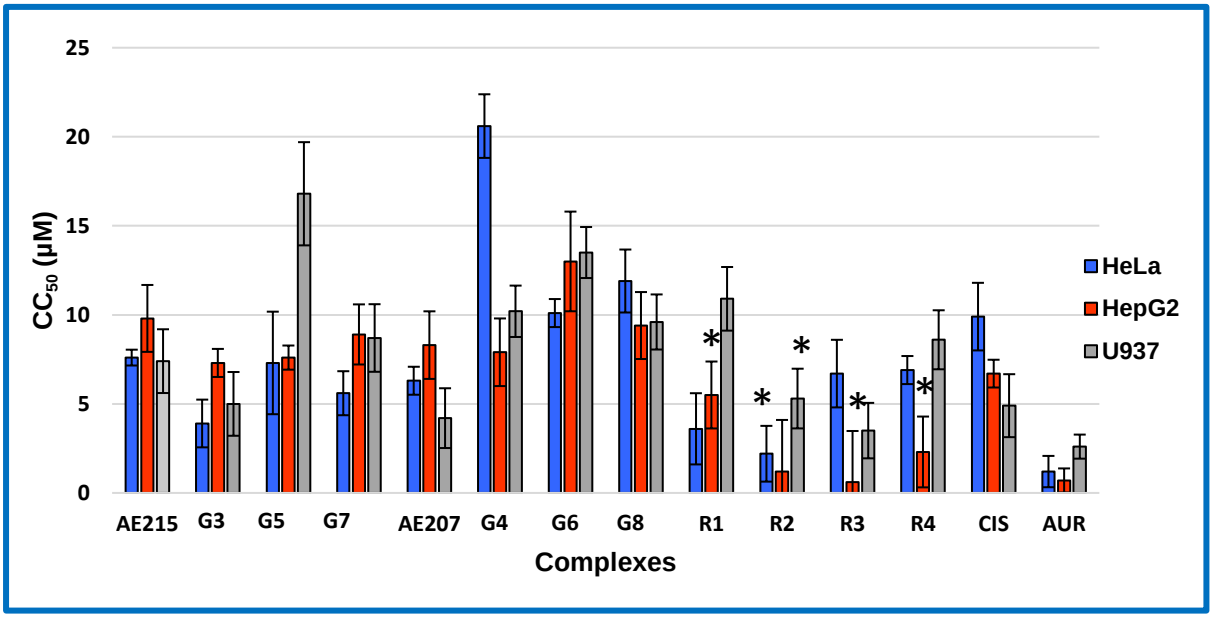

Figure 5: The CC_{50} values of the complexes across all cancer cell lines. *CC_{50} values of the metal complexes after 72-hour treatments across the three tested cancer cell lines. Complexes **G3**, **R2**, **R3**, and **R4** were more cytotoxic than their parent complexes respectively across all tested cancer cell lines. n=4, ±SEM, *(p<0.05).*

3.2 Complex selectivity index

An ideal drug is toxic to cancer cells and not toxic to noncancerous cells. Based on the literature, metal complexes should have SI values of greater than one indicates non-toxicity to noncancerous cells (Savic et al., 2016). After obtaining the CC_{50} of the complexes on all the three cancer cell lines, the selectivity for each complex was determined by diving the CC_{50} values obtained from treatments on Vero cells by the CC_{50} obtained from the cancerous cell lines in the study. For this, Vero cells were used for selectivity and these cell lines were treated with the complexes for 72 hours. The results obtained in ***Table 3*** showed that complexes **G3**, **G8**, **R3**, and **R4** had the desired SI values of above one across all cell lines. That meant that the four complexes were selective for the noncancerous cell line. The rest of the complexes were not selective for the noncancerous cell line. Also, complex **R1**, that showed selectivity against both HeLa and HepG2 cells was not selective against U937 cells. This shows that these complexes affected the three cancer cell lines differently.

Table 4: The SI values obtained after treatment on the Vero cell line. *Complexes* ***G3***, ***G8, R3***, *and* ***R4*** *had SI>1 showing that they are relatively selective against the noncancerous cell line.*

Complexes	HeLa	HepG2	U937
AE215	0.57	0.78	0.54
G3	1.23	1.66	1.97
G4	0.23	0.56	0.43
G5	0.84	0.93	0.42
G6	0.71	0.56	0.54
G7	0.76	0.48	0.49
G8	1.90	1.14	1.11
AE207	0.10	0.08	0.15
R1	1.48	2.77	0.61
R2	0.27	1.18	0.60
R3	1.18	2.52	2.24
R4	1.84	2.48	1.31
CIS	1.03	0.38	2.10
AUR	0.13	1.18	0.11

Based on the cytotoxicity and SI results, the complexes were inhibiting cancer cell progression where some of the complexes were selective against the noncancerous cells. Based on the literature review It was further investigated whether the manner of cell death shown in in the CC_{50} table was linked to any antioxidant activity. The study specifically focused on whether the complexes were able to act as free radical

scavengers and decrease the cellular NO concentration. For this, the DPPH and NO assay were chosen to test our hypothesis.

3.3 Radical scavenging activity using the DPPH assay

The DPPH assay (**Figure 6**) showed that none of the gold metal complexes exhibited any positive DPPH scavenging activity as their scavenging percentages were below 1%. The complexes **R2**, **R3**, and **R4** had positive DPPH scavenging with scavenging percentages of above 10% at complex concentrations of 25 µM and above. The DPPH scavenging was minimal when compared to the results of Vitamin C.

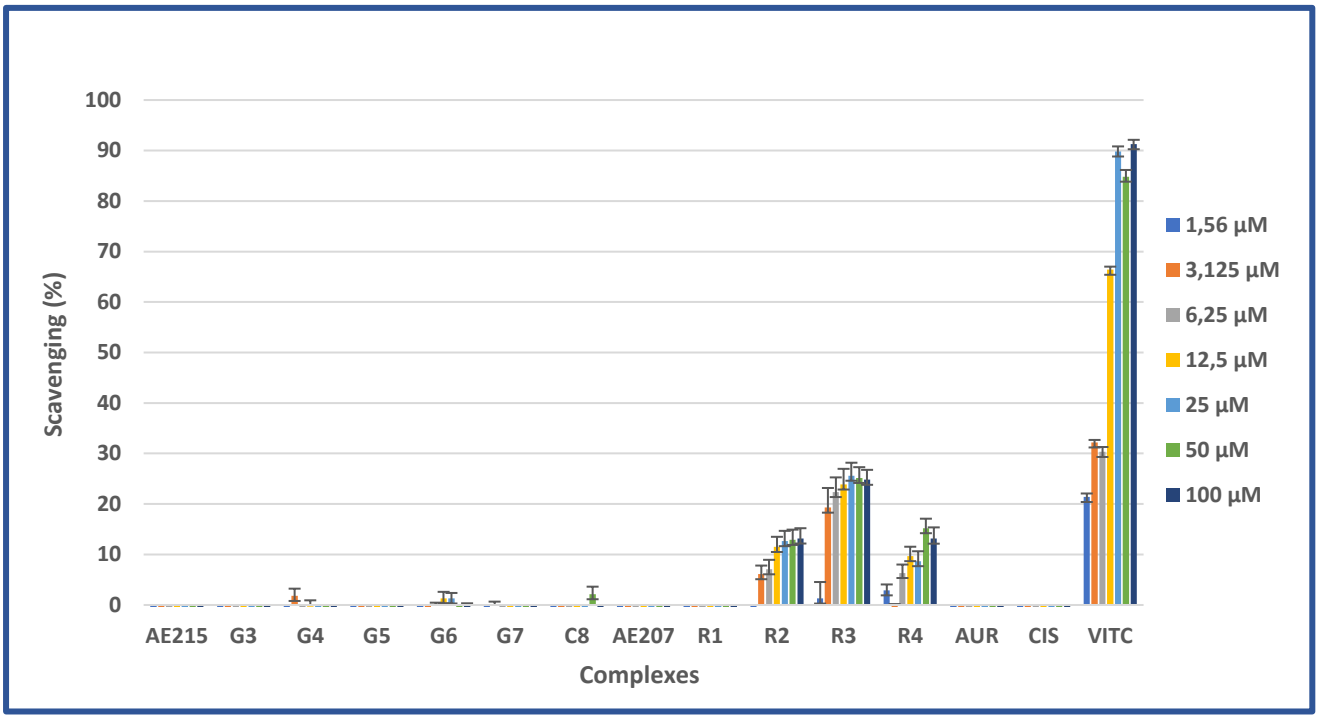

***Figure 6: DPPH scavenging**. Only the ruthenium complexes **R2**, **R3,** and **R4** showed DPPH scavenging above 10%. The gold complexes did not exhibit any positive DPPH scavenging after exposing the complexes to DPPH. n=4, ±SEM*

3.4 Antioxidant activity using the NO assay

The results obtained for NO inhibition at CC_{50} showed that the gold complexes **G3**, **G5**, and **G4** were able to decrease HeLa NO concentration to below 40 µM and the ruthenium complexes **R2**, **R3**, and **R4** decreased HeLa NO levels to below 20 µM after 72 hours of treatment (***Figure 7***). The complexes **G3**, **G5**, and **G7** were able to inhibit NO concentration better than their parent complex **AE215** across all cell lines resulting in NO concentrations of below 58 µM. Only complexes **G6** and **G8** were able to inhibit NO production better than the parent **AE207** was. The statistical analyses using the unpaired students T-test showed that the NO inhibition of these complexes was

significant when compared to untreated cells. The p-values of these complexes were all below 0.03.

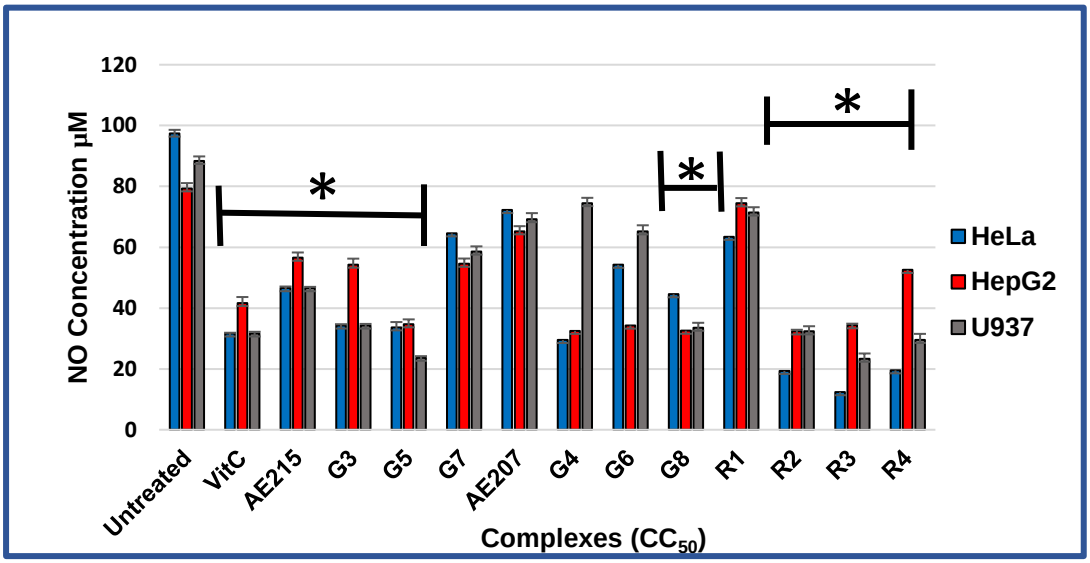

Figure 7: The NO inhibition levels at CC_{50}. *The complexes were all able to decrease cellular NO concentration where the ruthenium complexes R2, R3, and R4 were able to decrease NO production better than their parent complex and better than ascorbic acid indicating a similar mechanism of action to ascorbic acid. N=4, ±SEM, *(p≤0, 05),*

The complex concentrations were increased to $2XCC_{50}$ (***Figure 8***). It was then evaluated if increasing the complex concentration would also cause an increase in NO inhibition. As can be seen in the figure below, an increase in complex concentration caused a statistically significant decrease in NO concentration when compared to the untreated cells. The ruthenium complexes except **R1** had p-values of below 0.01. With the cellular NO below 25 µM in the presence of these complexes.

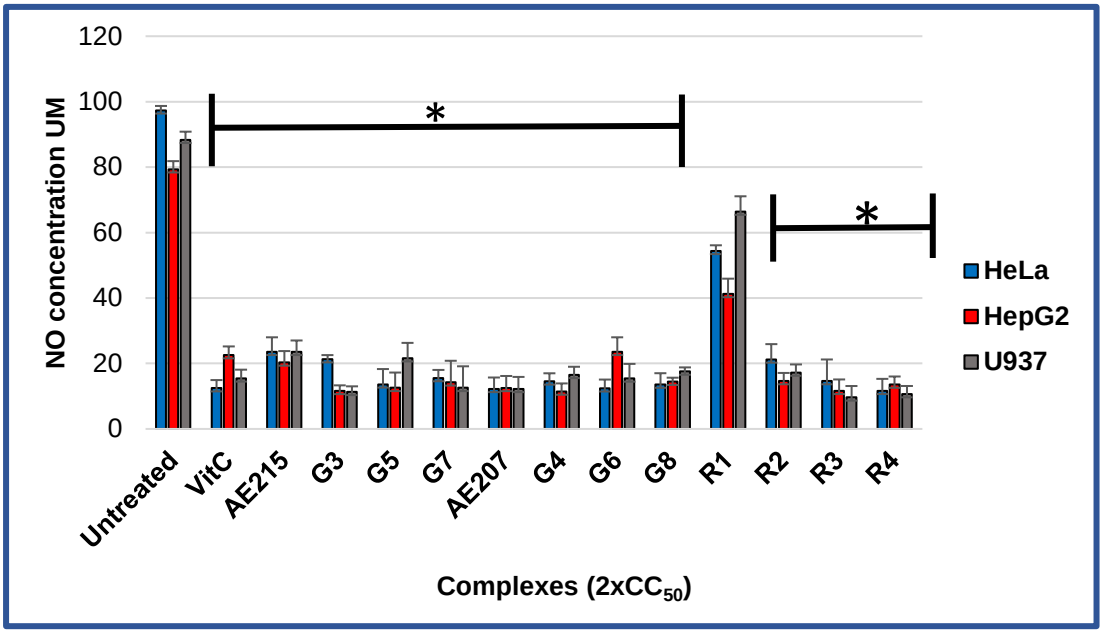

Figure 8: The NO inhibition levels at 2xCC$_{50}$. *Higher doses further decreased NO production to just under 20 µm concentration. The ruthenium complexes R2, R3, and R4 were able to reduce NO concentration better than the rest of the complexes. N=4, ±SEM, * (p≤0, 01).*

Based on the obtained results it was observed that the active metal complexes for the study were **G3**, **G8**, **R3**, and **R4** based on their CC$_{50}$, SI values, and their ability to inhibit NO concentration. These complexes were investigated further in the study for the induction of apoptosis.

3.5 Apoptosis-induction

After 72-hour treatments on HeLa cells the active complexes were able to induce apoptosis (***Figure 9)***. All the quadrant plats are in the Appendix III. In the presence of complex **G3,** 68% of the cells were in apoptotic phase while a percentage of 77% of HeLa cells were apoptotic in the presence of **G8**. A percentage of 69% of cells were apoptotic in the presence of **R3** and a percentage of 68% of cells were apoptotic in the presence of **R4**. The complex apoptosis-induction was statistically significant with p-values of below 0.01. All of the active complexes induced HeLa apoptosis better than cisplatin and Auranofin.

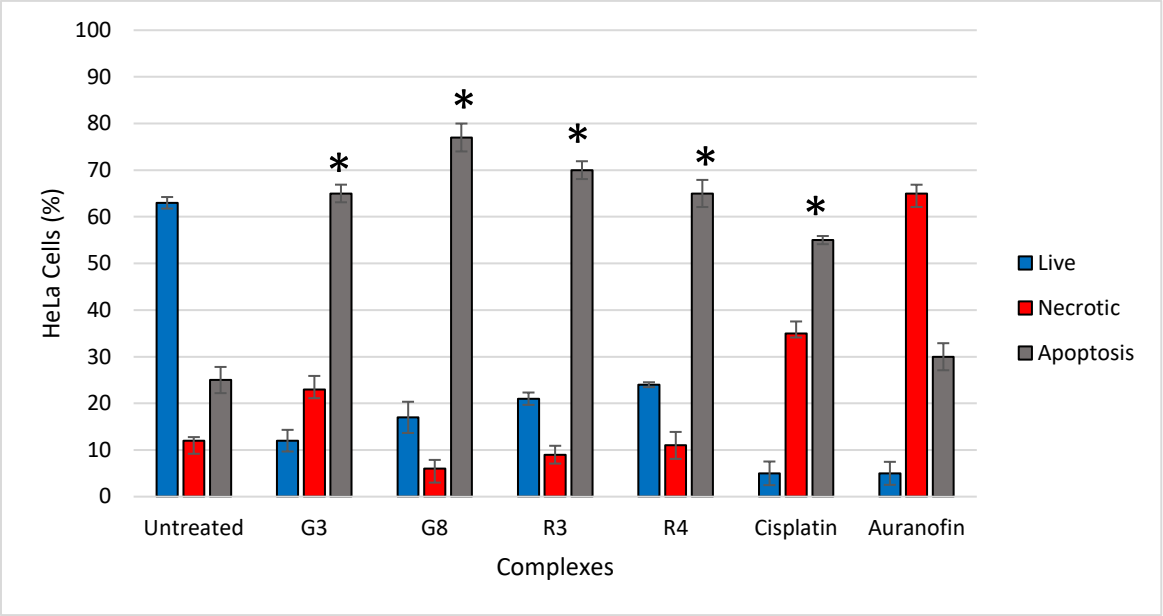

***Figure 9: Apoptosis induction in HeLa cells**: All of the complexes were able to induce apoptosis when compared to untreated cells. Auranofin resulted in mostly necrosis while complex **G8** induced the most apoptosis at 77% cells being apoptotic in the presence of this complex. N=4, ±SEM, *(p≤0, 01).*

After 72-hour treatments on Hepg2 cells the active complexes were able to induce apoptosis (***Figure 10***). A percentage of 72% of HepG2 cells were apoptotic after 72 hours of treatment with **G3** where 81% of cells were apoptotic after treatment with **G8**. A percentage of 67% cells were apoptotic when exposed to R3 and 79% cells were apoptotic after treatment with **R4**. The complexes induced apoptosis better than cisplatin and Auranofin. The statistical evaluation that the apoptosis induction was statistically significant with p-values of below 0.01 compared to the untreated cells.

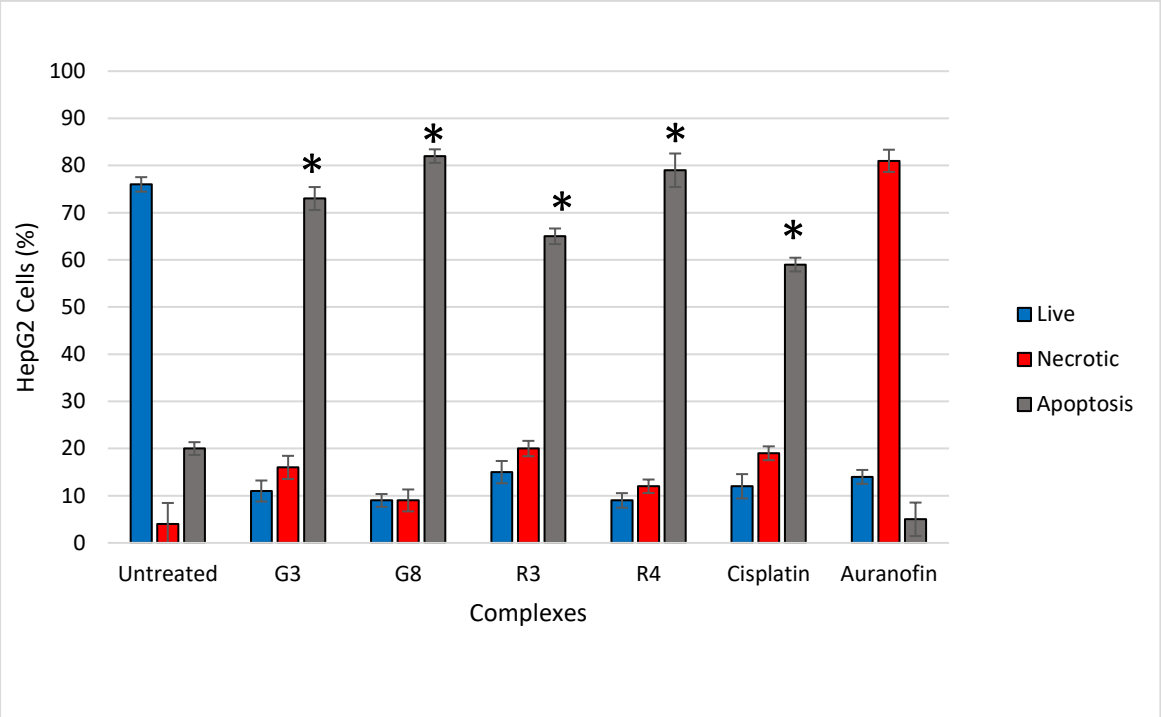

Figure 10: Apoptosis induction in HepG2 cells*. The above-figure shows the results obtained after treating HepG2 cells with the active complexes for 72 hours. The untreated cells were still alive (blue) and the cells were apoptotic (gravy) in the presence of the active complexes. Complex **G8** induced the most apoptosis in these cell lines. N=4, ±SEM, * (p≤0, 01).*

Lastly, the U937 cells were treated with the active complexes for apoptosis-induction (***Figure 11***). Compared to untreated cells, all of the cells were in an apoptotic phase in the presence of the active complexes. A percentage of 69% cells were apoptotic in the presence of **G3**, 79% cells were apoptotic in the presence of **G8**, and 88% cells were apoptotic in the presence of **R3**. A percentage of 66% cells were apoptotic in the presence of **R4**. The apoptosis-induction was statistically significant with p-values of below 0.01 for all the active complexes.

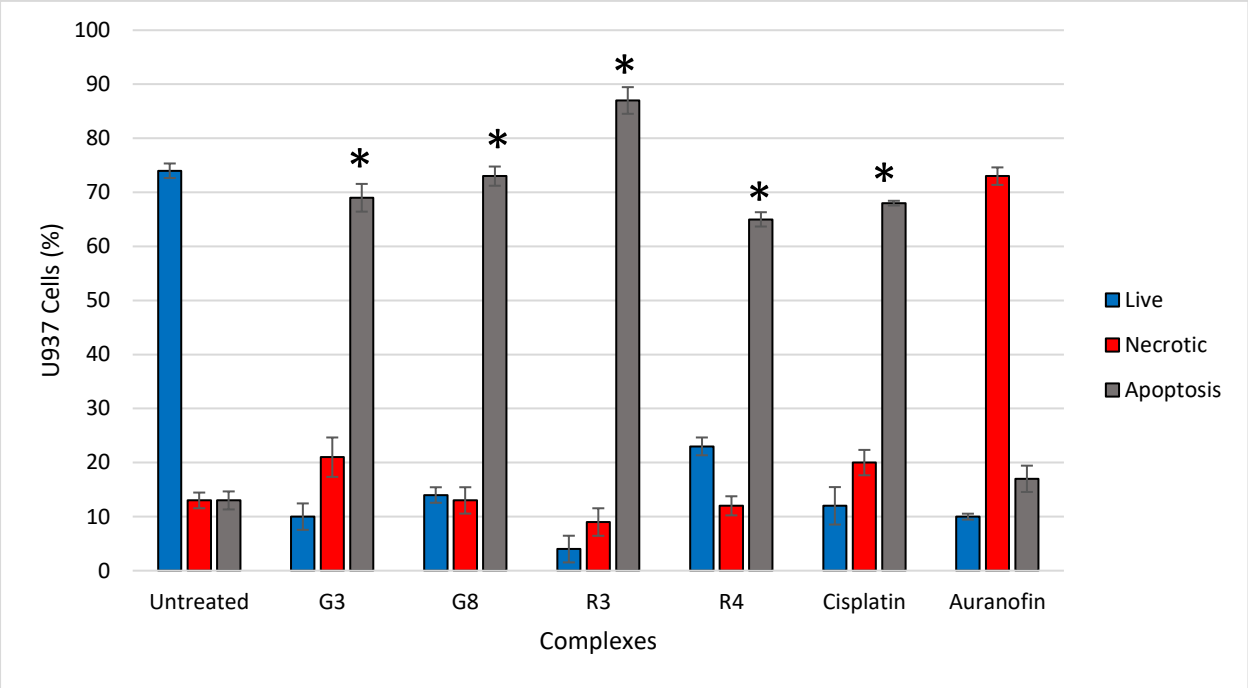

***Figure 11: Apoptosis induction in U937 cells**.: The above image shows the apoptosis results obtained after treating U937 cells with active metal complexes. When comparing untreated cells and cells treated with the active complexes, it was seen that all of the active complexes were able to induce apoptosis. N=4, ±SEM, * (p≤0, 01).*

The next step was to determine the drug-likeness of the metal complexes used in our study.

3.6 Molecular Drug-likeness predictions using Molinspiration

The Molinspiration software was used to compute the molecular properties of each complex as based on Lipinski's Rule of Five. The only complexes that abided by all the stipulated rules are complexes **AE215** and **AE207 (Table 4).** Complex **AE215** had a molecular weight of 461.68 g/mol, LogP value of 0.41, 2 hydrogen donors, one hydrogen acceptor, a TPSA of 26.02, and 5 rotatable bonds. Complex **AE207** had a molecular weight of 475.71 g/mol, a LogP value of 0.69, 2 hydrogen donors, one hydrogen acceptor, a TPSA of 26.02, and 6 rotatable bonds. Most of the tested complexes had molecular weights above 500 g/mol. Only the gold complexes had logP values below five while the ruthenium complexes had logP values above nine. Most of the complexes had hydrogen donors below five except complexes **G3** and **G4** with seven hydrogen donors each. Most of the complexes had hydrogen accepters below 10 except complexes **G5**, **G6**, **G7**, and **G8, which** had more than 11 hydrogen acceptors. None of the tested metal complexes had rotatable bonds lower than five except **AE215** and **AE2017**.

***Table 5**: **Molecular drug-likeness of the tested metal complexes obtained using Molinspiration**. The complexes highlighted in red are the active complexes which were evaluated in the apoptosis assay.*

Name	MW	logP	H Donors	H Acceptors	TPSA	Rotatable bonds
AE215	461.68	0.41	2	1	26.02	5
G3	640.83	-1.65	7	7	134.82	11
G4	654.86	-1.38	7	7	134.82	12
G5	851.02	1.44	2	12	165.20	21
G6	865.04	1.70	2	12	165.20	22
G7	891.71	-1.22	4	13	191.22	23
G8	905.73	-0.95	4	13	191.22	24
AE207	475.71	0.69	2	1	26.02	6
R1	869.00	9.65	0	6	59.09	21
R2	1126.14	10.09	0	4	32.78	20
R3	1418.32	10.52	0	4	32.78	19
R4	1503.40	10.65	0	6	59.09	26
Aur	679.49	1.407	0	10	134.68	14
CIS	300.05	-2.83	4	2	52.05	0

CHAPTER 4: DISCUSSION

Chemotherapy and radiation therapy can cause long-term side effects on the brain, spinal cord, and nerves (Blanchard et al., 2015). These side effects include Hearing loss from high doses of chemotherapy, especially of drugs like cisplatin (Haugnes et al., 2018). The main objective of this research was to study potential drug leads that could act against multiple types of cancers. Eight gold complexes (**AE215**, **AE207**, **G3**, **G4**, **G5**, **G6**, **G7**, and **G8**) and four ruthenium complexes (**R1**, **R2**, **R3**, and **R4**) were tested on cervical cancer, liver cancer, and leukaemia. To facilitate cell entry, the derived gold metal complexes contained glucose molecules where we expected the complexes to be easily taken up by the cellular glucose-sodium symporter which forms part for the cells' active transport mechanism of cell entry (Gorraitz et al., 2017).. Although metal complexes are being investigated as probes and therapeutics, there are relatively few studies on their mechanism of uptake. The main routes into a cell are either endocytosis, active transport, facilitated diffusion, and passive diffusion (O'donoghue et al., 2016). The cellular accumulation of cisplatin has received the most scrutiny and has been recently reviewed where platinum drugs were shown to enter the cell by passive diffusion through organic cation transporters such as the copper transporter Ctr1. It has also previously been shown that upon cell entry, ruthenium complexes accumulate in the cell cytoplasm. Cellular uptake of some ruthenium (III) complexes appear to be mediated by the iron transport protein transferrin. KP1019 (indazolium trans- [tetrachlorobis (1H-indazole) ruthenate (III)]) binds transferrin with the displacement of a chloride ligand and is transported into cells with transferrin by receptor-mediated endocytosis. Ruthenium complexes lacking a labile ligand such as chloride are unlikely to be able to enter cells in this manner, and their mechanism of entry has not been established.

4.1 Complex cytotoxicity

The chemical structure of a drug determines its physicochemical properties, its ADME/Tox properties, and ultimately affects its pharmacological activity. Medicinal chemists can regulate the pharmacological activity of drug molecules by modifying the structure. The first step in testing our hypothesis was to determine the CC_{50} of our complexes. The parent complexes were compared to their derivatives. In HeLa cells, **G3** was more cytotoxic to **AE215**. Comparing their structures shows that **G3** is not only larger in length that **AE215** but it also has hydroxyl functional groups attached to

it. The chemical properties of OH groups include being able to form intermolecular interactions with water, high polarity, and increased solubility in organic solvents, which might have led to the complex being more toxic to the HeLa cells compared to **AE215**. The complexes were dissolved in DMSO, therefore, **G3** may have dissolved better than the parent complex facilitating a better uptake by HeLa cells compared to **AE215,** resulting in a decrease in the viability of these cells. Additionally, since HeLa cells are adherent a complex that easily dissolves increases the cytotoxic surface area (Krishnamoorthy et al., 2011).

Complex **AE207** was more cytotoxic than its derivatives. This could be linked to its size as smaller complexes diffuse readily into the lipid bilayer.

The ruthenium complex **R2** was the most cytotoxic of the ruthenium complexes. When comparing their structures to the ligand **R1** we could see that the presence of the metal (***Table 2***) greatly influences its activity. The ruthenium complexes have benzene rings, and this makes them to biochemically possess delocalized pi-electrons leading to lower overall energy of the molecules, making them more stable (Frasca et al., 1996).

When comparing **R3** (trans-) and **R4** (cis) ruthenium complexes we could already see that there was a difference in their cytotoxicity (***Figure 5***). This phenomenon is not entirely new as cisplatin and transplatin have been shown to be different in their activity as well. Transplatin produces much fewer DNA adducts than cisplatin but both have been shown to be cytotoxic causing DNA restriction when attacking cells (Bernal-Méndez et al., 1997). In transplatin, the leaving groups, which are two Cl- ions, are in trans position and cannot perform well as compared to the leaving Cl- ions of cisplatin. With that said, our results showed that the trans- ruthenium complex was on the contrary more cytotoxic than the cis conformation complex. This could be because none of the transition group metal behave the same. Just because cisplatin or its derivatives behaved in a certain manner, we could not assume that our ruthenium complexes would also behave the same. Therefor this was the first time that it was reported that these novel ruthenium complexes behaved in this manner.

Generally, the ruthenium complexes were more cytotoxic than the gold complexes. This cytotoxicity could be linked to the logP and TPSA values of these complexes. Larger molecules do not have difficulty in crossing the cell membrane and they have been shown to bind tighter to their molecular targets (Bouet and Funnel., 2000). Upon

cell entry, these complexes could be binding to key cellular elements like tubulins, microtubules and these bindings could be strong enough to stop mitosis.

In the drug discovery process, drug candidates are screened not only for cytotoxicity but also for selectivity. The selectivity index of a compound is a widely accepted parameter used to express the *in vitro* efficacy of the compound in the inhibition of cancer progression. As previously mentioned, an ideal drug must have a high SI (Kissin., 2013). From the results obtained only complexes **G3**, **G8**, **R3**, and **R4** had high selectivity for all cancer cell lines (SI >1). This basically means that based on these results these complexes are very suitable to be used in chemotherapy as they would not harm the patient with adverse side effects. The complexes would generally target the cancerous cells more than the healthy cells.

4.2 Antioxidant activity using the DPPH assay

The hypothesis of the study was tested by evaluating the DPPH-scavenging ability of the complexes. After analysing the DPPH-scavenging results (***Figure 6***) it was seen that none of the gold complexes showed any positive DPPH scavenging ability above 10%. The ruthenium complexes showed minimal DPPH-scavenging ability where **R3** showed the highest scavenging ability. Since the DPPH assay is a cell-free assay the inactivity of the gold complexes is linked to their oxidation state where gold complexes have been previously shown to be inactive when exposed to DPPH (Tzeng., 2004).

4.3 Antioxidant activity using the NO assay

After obtaining the CC_{50} of the complexes, the hypothesis of the study was tested further by determining if the complexes were able to inhibit cellular NO production and this was to try to link it to apoptosis. The results showed that all the complexes were able to inhibit NO levels in cancer cells. On a biochemical level, NO inhibition is linked to mitochondrial activity where high levels of NO actively inhibit cytochrome c oxidase leading to decreased respiration, increasing cancer progression (Brown., 2001). Cytochrome c links both the NO inhibition part of the study to the apoptosis section because cytochrome c can function as an activator of the intrinsic pathway of apoptosis (Yang et al., 2011). Our complexes could be directly or indirectly interacting with the nitric oxide synthase pathway where they could be L-Arginine inhibitors. The complexes could be taken up by the mitochondria and interacts with mitochondrial DNA or mitochondrial proteins, or even initiate mitochondrial-dependent cell death signalling by unbalancing the cellular redox state (Tomas-Gamasa et al., 2016).

4.4 Apoptosis-induction

Four complexes were selected from the initial group of complexes based on their acceptable CC_{50} and SI values (give the table reference here) and these were investigated for their ability to induce apoptosis in all three cancer cell lines. This was conducted because as previously mentioned the evasion of apoptosis is linked to cancer progression. It was previously reported by Srdić-Rajić et al 2011 that metal complexes induce apoptosis in cancer cells via activation of the mitochondrial pathway in a time- and dose-dependent manner; and result in changes in the cell-cycle distribution of cells. The results obtained upon treatment of cancer cells for 72 hours show that the selected complexes indeed exerted their anticancer activity through the induction of apoptosis. The two ruthenium complexes (**R3** and **R4**) were able to induce apoptosis the most. At this point in the research it cannot be concluded whether the apoptosis seen is via the intrinsic or extrinsic pathway. However, if the complexes induce apoptosis via the intrinsic pathway, the complexes could be binding or interacting with the mitochondria to activate the pro-apoptotic proteins leading to the release of cytochrome c. If the complexes induce apoptosis via the extrinsic pathway the complexes could be binding to and activating the death receptors on the death domains. These results correlate to the findings by Chen et al, 2011 where the researchers demonstrated that $[Ru(phen)_2\text{-p-MOPIP}](PF_6)_2 \cdot 2H_2O$ (RuPOP), a ruthenium complex with potent antiproliferative activity, was able to induce mitochondria-mediated and caspase-dependent apoptosis in human cancer cells compared to the other tested metal complexes including gold complexes. Based on these results, we hypothesise that our complexes cause apoptosis by interacting with the NO signalling pathway because as seen from the results, a clear trend was seen showing that the complexes that reduced the most NO production (***Figure 7*** *a*nd ***8***) during cancer progression induced the most apoptosis (***Figures 9, 10,*** and ***11***).

4.5 Molecular drug-likeness

We used Molinspiration to evaluate the drug-likeness of our complexes. Based on the results obtained in our study we could see that complexes **AE215** and **AE207** were the only complexes that abided by all five of Lipinski's rules. This means that these complexes were not only just water-soluble but they also had faster absorption and action due to not having too many hydrogen bond donors. Complexes **G3** and **G4** had MW>500 however, it has been shown that complexes that have MW<700 also readily

diffuse through the cell membrane (Nama et al., 2005). Both complexes had low logP values, low hydrogen-bond acceptors, and PSA values of less than 140 making these complexes soluble in water and fat. These complexes would be ideal for oral administration as they would be able to pass through the intestinal lining after consumption and be carried to aqueous blood and penetrate the lipid-based cell membrane to reach the inside of the cell (Sharma et al., 2011). Complexes **G4**, **G5**, **G6**, **G7**, and **G8** have high MW rendering them difficult to diffuse through the cell membrane. The complexes have low logP values and low hydrogen bond donors meaning that they are actively absorbed upon administration. The complexes are also lipophylic. The ruthenium complexes are regarded as large molecules (MW>700 g/mol) and in principle, this makes these complexes difficult to passively diffuse into the cell membrane. However, these complexes have exceptionally low hydrogen bond donor's PSA values meaning that they are actively absorbed and have good oral bioavailability. There is several drugs currently in clinical usage and available on the market which also do not abide by all five rules, Auranofin is an example of such drugs (**Table 4**). This shows that the rule of five may not necessarily be used as a stringent drug disqualifier, but rather as a guide in the broader drug discovery pipeline

CHAPTER 5: CONCLUSION AND FUTURE PERSPECTIVES

In conclusion, six gold and three ruthenium complexes were successfully synthesized, and their anticancer activity were tested on HeLa, U937, and HepG2 cells. These complexes were then compared to their parent complexes. **G3**, **G6**, and **R4** of the complexes were selective against cancer cells when treated against the mammalian Vero cell line. The DPPH scavenging ability of the complexes was very weak, and the NO inhibition results obtained on just two concentrations were not enough to give conclusions, but the results give an idea of the potential antioxidant ability of the complexes

Furthermore, three of the complexes with NO inhibition were able to induce apoptosis better than its parent complex in all the tested cancer cell lines. This indicates the potency of the complex and indicating that modifications of the complex structure ultimately influence its activity.

The active complexes were able to induce apoptosis where the ruthenium complexes showed better apoptosis-inducing ability better than the gold complexes

The future perspectives of the study include determining the specific protein-drug interactions, to fully understand the complexes' mechanism of anticancer activity. These proteins would be the proteins of the intrinsic apoptotic pathway (BCL-2 proteins). By determining the protein expression levels of these proteins in the presence and absence of the complexes we could then make more definitive conclusions as to what the mechanism of action is of the complexes in the study. The same method could be carried out by determining the expression of Cyt-c both in the presence and absence of the metal complexes. These finding would be able to link all the results obtained in the study in order to tell a better more substantiated narrative.

ANSWERS TO RESEARCH QUESTIONS

The alternative hypothesis of this study was that "*Gold and ruthenium complexes should have in vitro anti-cancer activity with significant antioxidant and apoptosis-induction activity.*" In order to test this hypothesis a number of research questions were posed. Responses to these questions are provided below.

Can the metal complexes inhibit the viability of HeLa (cervical cancer), U937 (Leukaemia), and HepG2 (liver cancer) cells?

All of the tested complexes were able to inhibit cancer cell viability. Where the gold complexes **G3** and **G6** and the ruthenium complex **R4** inhibited HeLa cell viability better than their parent complexes at the lowest tested concentrations (0.78 µM). In HepG2 cancer cells, the complexes **G4**, **G5**, and **R3** were able to inhibit cancer viability better than their parent complexes respectively. Complexes **G3**, **G6**, and **R4** were able to inhibit U937 cell viability better than their parent complexes respectively. This led to the realization that these complexes are cancer-specific and might have different mechanisms of anticancer action.

What are the CC_{50} values of these complexes on the tested cancer cell lines?

The complexes varied in their level of cytotoxicity in all tested cancer cell lines. Complexes **G3**, **G7**, and all the ruthenium complexes were the most cytotoxic to HeLa cells with (CC_{50}<7 µM). These complexes were more cytotoxic than cisplatin. The treatment results obtained on U937 cells show that the complexes **G3**, **G5**, and the ruthenium complexes were more cytotoxic against this cell line. Complexes **G3**, **G4**, and the ruthenium complexes were cytotoxic against HepG2 cells. These results showed how complex **G3** and the ruthenium complexes remained consistent in their cytotoxicity across all the tested cell lines.

Are the complexes selective against non-cancerous mammalian cells?

The complexes were toxic to the tested cancer cells as seen by their ability to decrease cancer cell viability. However, only complexes **G3**, **G8**, **R3**, and **R4** were selective against the noncancerous Vero cell line with SI values above one.

Do the complexes have antioxidant activity?

None of the gold metal complexes had positive DPPH scavenging ability meaning that their activity is dependent on the complexes interacting with a specific molecular target inside the cancer cells. The ruthenium complexes **R2**, **R3**, and **R4** had positive DPPH-scavenging activity indicating that there can act as antioxidants regardless of cellular interactions. All the active complexes were able to reduce cellular NO production across all cancer cell lines, indicating that not only can the complexes inhibit cancer cell viability, but there can reduce cell ROS production too.

Are the complexes able to induce cell apoptosis?

All of the active metal complexes were able to induce cell apoptosis across all cell lines.

What is the overall drug like-ness of the complexes?

Unfortunately, none of the modified complexes abided by all five of the rules of drug-likeness as they only abided by 3 of the rules. However, this does not disqualify them completely from being pursued further for their anticancer activities, as many of the currently used drugs in the market do not abide by all five rules.

Finally, the current use of metal complexes in medicine reveals the extensive potential for metal complexes. The significant identification of complexes, which are cytotoxic to cancer cells and non-toxic to non-cancerous cells show the potential of these complexes in the chemotherapeutic drug pipeline. All of these complexes were able to reduce cancer ROS production by the inhibition of NO supporting the hypothesis of this study.

CHAPTER 6: REFERENCES

Adam, R., Alberico, E., Baumann, W., Drexler, H.J., Jackstell, R., Junge, H. and Beller, M., 2016. NNP-Type Pincer Imidazolylphosphine Ruthenium Complexes: Efficient Base-Free Hydrogenation of Aromatic and Aliphatic Nitriles under Mild Conditions. Chemistry–A European Journal, 22(14), pp.4991-5002.

Adamson, E.D., 1987. Oncogenes in development. Development, 99(4), pp.449-471.

Agonigi, G., Riedel, T., Zacchini, S., Păunescu, E., Pampaloni, G., Bartalucci, N., Dyson, P.J. and Marchetti, F., 2015. Synthesis and Antiproliferative Activity of New Ruthenium Complexes with Ethacrynic-Acid-Modified Pyridine and Triphenylphosphine Ligands. Inorganic chemistry, 54(13), pp.6504-6512.

Amore, B.M., Gibbs, J.P., and Emery, M.G., 2010. Application of in vivo animal models to characterize the pharmacokinetic and pharmacodynamic properties of drug candidates in discovery settings. Combinatorial chemistry & high throughput screening, 13(2), pp.207-218.

Arbyn, M., Snijders, P.J., Meijer, C.J., Berkhof, J., Cuschieri, K., Kocjan, B.J. and Poljak, M., 2015. Which high-risk HPV assays fulfill criteria for use in primary cervical cancer screening? Clinical Microbiology and Infection, 21(9), pp.817-826.

Bergamo, A. and Sava, G., 2015. Linking the future of anticancer metal-complexes to the therapy of tumor metastases. Chemical Society Reviews, 44(24), pp.8818-8835.

Bergquist, A. and von Seth, E., 2015. Epidemiology of cholangiocarcinoma. Best practice & research Clinical gastroenterology, 29(2), pp.221-232.

Bernal-Méndez, E., Boudvillain, M., González-Vílchez, F. and Leng, M., 1997. Chemical versatility of transplatin monofunctional adducts within multiple site-specifically platinated DNA. Biochemistry, 36(24), pp.7281-7287.Bian, C., Yao, K., Li, L., Yi, T. and Zhao, X., 2016. Primary debulking surgery vs. neoadjuvant chemotherapy followed by interval debulking surgery for patients with advanced ovarian cancer. Archives of gynecology and obstetrics, 293(1), pp.163-168.

Beurel, E. and Jope, R.S., 2006. The paradoxical pro-and anti-apoptotic actions of GSK3 in the intrinsic and extrinsic apoptosis signaling pathways. Progress in neurobiology, 79(4), pp.173-189.

Bidovec, K., Božič, J., Dolenc, I., Turk, B., Turk, V. and Stoka, V., 2017. Tumor Necrosis Factor-α Induced Apoptosis in U937 Cells Promotes Cathepsin D-Independent Stefin B Degradation. Journal of cellular biochemistry, 118(12), pp.4813-4820.

Blanchard, P., Lee, A., Marguet, S., Leclercq, J., Ng, W.T., Ma, J., Chan, A.T., Huang, P.Y., Benhamou, E., Zhu, G. and Chua, D.T., 2015. Chemotherapy and radiotherapy in nasopharyngeal carcinoma: an update of the MAC-NPC meta-analysis. The lancet oncology, 16(6), pp.645-655.

Bouet, J.Y., Surtees, J.A. and Funnell, B.E., 2000. Stoichiometry of P1 plasmid partition complexes. Journal of Biological Chemistry, 275(11), pp.8213-8219.

Boyd, M.R. and Paull, K.D., 1995. Some practical considerations and applications of the National Cancer Institute in vitro anticancer drug discovery screen. Drug Development Research, 34(2), pp.91-109.

Bragin, A.O., Saik, O.V., Chadaeva, I.V., Demenkov, P.S., Markel, A.L., Orlov, Y.L., Rogaev, E.I., Lavrik, I.N. and Ivanisenko, V.A., 2017. Role of apoptosis genes in aggression revealed using combined analysis of System gene networks, expression and genomic data in grey rats with aggressive behavior. Vavilovskii Zhurnal Genetiki i Selektsii, 21(8), pp.911-919.

Brown, G.C., 2001. Regulation of mitochondrial respiration by nitric oxide inhibition of cytochrome c oxidase. Biochimica et Biophysica Acta (BBA)-Bioenergetics, 1504(1), pp.46-57.

Cantara, S., Capezzone, M., Marchisotta, S., Capuano, S., Busonero, G., Toti, P., Di Santo, A., Caruso, G., Carli, A.F., Brilli, L. and Montanaro, A., 2010. The impact of proto-oncogene mutation detection in cytological specimens from thyroid nodules improves the diagnostic accuracy of cytology. The Journal of Clinical Endocrinology & Metabolism, 95(3), pp.1365-1369.

Chang, S.W., Lewis, A.R., Prosser, K.E., Thompson, J.R., Gladkikh, M., Bally, M.B., Warren, J.J. and Walsby, C.J., 2016. CF3 derivatives of the anticancer Ru (III) complexes KP1019, NKP-1339, and their imidazole and pyridine analogs show

enhanced lipophilicity, albumin interactions, and cytotoxicity. Inorganic chemistry, 55(10), pp.4850-4863.

Che, C.M. and Siu, F.M., 2010. Metal complexes in medicine with a focus on enzyme inhibition. Current opinion in chemical biology, 14(2), pp.255-261.

Chen, T., Liu, Y., Zheng, W.J., Liu, J. and Wong, Y.S., 2010. Ruthenium polypyridyl complexes that induce mitochondria-mediated apoptosis in cancer cells. Inorganic chemistry, 49(14), pp.6366-6368.

Chen, M., Vijay, V., Shi, Q., Liu, Z., Fang, H. and Tong, W., 2011. FDA-approved drug labelling for the study of drug-induced liver injury. Drug discovery today, 16(15-16), pp.697-703.

Chiribella, G., 2012. Perfect discrimination of no-signalling channels via quantum superposition of causal structures. Physical Review A, 86(4), p.040301.

Coghill, A.E., Shiels, M.S., Suneja, G. and Engels, E.A., 2015. Elevated cancer-specific mortality among HIV-infected patients in the United States. Journal of Clinical Oncology, 33(21), p.2376.

Crowley, L.C., Marfell, B.J., Scott, A.P. and Waterhouse, N.J., 2016. Quantitation of apoptosis and necrosis by annexin V binding, propidium iodide uptake, and flow cytometry. Cold Spring Harbor Protocols, 2016(11), pp.pdb-prot087288.

Dasari, S. and Tchounwou, P.B., 2014. Cisplatin in cancer therapy: molecular mechanisms of action. European journal of pharmacology, 740, pp.364-378.

De Luca, A., Parker, L.J., Ang, W.H., Rodolfo, C., Gabbarini, V., Hancock, N.C., Palone, F., Mazzetti, A.P., Menin, L., Morton, C.J. and Parker, M.W., 2019. A structure-based mechanism of cisplatin resistance mediated by glutathione transferase P1-1. Proceedings of the National Academy of Sciences, 116(28), pp.13943-13951.

de Martel, C., Plummer, M., Vignat, J. and Franceschi, S., 2017. Worldwide burden of cancer attributable to HPV by site, country, and HPV type. International journal of cancer, 141(4), pp.664-670.

DeNicola, G.M., Karreth, F.A., Humpton, T.J., Gopinathan, A., Wei, C., Frese, K., Mangal, D., Kenneth, H.Y., Yeo, C.J., Calhoun, E.S. and Scrimieri, F., 2011. Oncogene-induced Nrf2 transcription promotes ROS detoxification and tumorigenesis. Nature, 475(7354), p.106.

Dharmaraj, N., Viswanathamurthi, P. and Natarajan, K., 2001. Ruthenium (II) complexes containing bidentate Schiff bases and their antifungal activity. Transition Metal Chemistry, 26(1-2), pp.105-109.

Duan, D., Zhang, J., Yao, J., Liu, Y. and Fang, J., 2016. Targeting thioredoxin reductase by parthenolide contributes to inducing apoptosis of HeLa cells. Journal of Biological Chemistry, 291(19), pp.10021-10031.

Duffy, B.C., Zhu, L., Decornez, H. and Kitchen, D.B., 2012. Early phase drug discovery: cheminformatics and computational techniques in identifying lead series. Bioorganic & medicinal chemistry, 20(18), pp.5324-5342.

Fiskus, W., Saba, N., Shen, M., Ghias, M., Liu, J., Gupta, S. D., Bhalla, K. N. (2014). Auranofin Induces Lethal Oxidative and Endoplasmic Reticulum Stress and Exerts Potent Preclinical Activity against Chronic Lymphocytic Leukemia. Cancer Research, 74(9), 2520–2532.

Florea, A.M. and Büsselberg, D., 2011. Cisplatin as an anti-tumour drug: cellular mechanisms of activity, drug resistance, and induced side effects. Cancers, 3(1), pp.1351-1371.

Ford, P.C., and Lorkovic, I.M., 2002. Mechanistic aspects of the reactions of NO with transition-metal complexes. Chemical Reviews, 102(4), pp.993-1018.

Frasca, D., Ciampa, J., Emerson, J., Umans, R.S. and Clarke, M.J., 1996. Effects of hypoxia and transferrin on toxicity and DNA binding of ruthenium antitumor agents in HeLa cells. Metal-Based Drugs, 3(4), pp.197-209.

Fu, D., Calvo, J.A. and Samson, L.D., 2012. Balancing repair and tolerance of DNA damage caused by alkylating agents. Nature Reviews Cancer, 12(2), p.104.

Fukumura, D., Kashiwagi, S. and Jain, R.K., 2006. The role of nitric oxide in tumour progression. Nature Reviews Cancer, 6(7), pp.521-534.

Fulda, S. and Debatin, K.M., 2006. Extrinsic versus intrinsic apoptosis pathways in anticancer chemotherapy. Oncogene, 25(34), pp.4798-4811.

Galluzzi, L., Vitale, I., Michels, J., Brenner, C., Szabadkai, G., Harel-Bellan, A., Castedo, M. and Kroemer, G., 2014. Systems biology of cisplatin resistance: past, present, and future. Cell death & disease, 5(5), p.e1257.

Gama, N., Kumar, K., Ekengard, E., Haukka, M., Darkwa, J., Nordlander, E. and Meyer, D., 2016. Gold (I) complex of one, 1′-bis (diphenylphosphino) ferrocene–quinoline conjugate: a virostatic agent against HIV-1. BioMetals, 29(3), pp.389-397.

Garcia-Belinchón, M., Sánchez-Osuna, M., Martínez-Escardó, L., Granados-Colomina, C., Pascual-Guiral, S., Iglesias-Guimarais, V., Yuste, V. J. (2015). An Early and Robust Activation of Caspases Heads Cells for a Regulated Form of Necrotic-like Cell Death. The Journal of Biological Chemistry, 290(34), 20841–20855.

Gerlier, D. and Thomasset, N., 1986. Use of MTT colorimetric assay to measure cell activation. Journal of immunological methods, 94(1-2), pp.57-63.

Gill, M.R. and Vallis, K.A., 2019. Transition metal compounds as cancer radiosensitizers. Chemical Society Reviews, 48(2), pp.540-557.

Goldar, S., Khaniani, M.S., Derakhshan, S.M. and Baradaran, B., 2015. Molecular mechanisms of apoptosis and roles in cancer development and treatment. Asian Pac J Cancer Prev, 16(6), pp.2129-2144.

Gorraitz, E., Hirayama, B.A., Paz, A., Wright, E.M. and Loo, D.D., 2017. Active site voltage-clamp fluorometry of the sodium-glucose cotransporter hSGLT1. Proceedings of the National Academy of Sciences, 114(46), pp. E9980-E9988.

Graf, N., & Lippard, S. J. (2012). Redox activation of metal-based prodrugs as a strategy for drug delivery. Advanced Drug Delivery Reviews, 64(11), 993–1004.

Green, D. R., & Llambi, F. (2015). Cell Death Signaling. Cold Spring Harbor Perspectives in Biology, 7(12), a006080.

Harbut, M. B., Vilchèze, C., Luo, X., Hensler, M. E., Guo, H., Yang, B., Wang, F. (2015). Auranofin exerts broad-spectrum bactericidal activities by targeting thiol-redox

homeostasis. Proceedings of the National Academy of Sciences of the United States of America, 112(14), 4453–4458. http://doi.org/10.1073/pnas.1504022112.

Hargrove, A. E., Martinez, T. F., Hare, A. A., Kurmis, A. A., Phillips, J. W., Sud, S., Dervan, P. B. (2015). Tumour Repression of VCaP Xenografts by a Pyrrole-Imidazole Polyamide. PLoS ONE, 10(11), e0143161.

Haugnes, H.S., Stenklev, N.C., Brydøy, M., Dahl, O., Wilsgaard, T., Laukli, E. and Fosså, S.D., 2018. Hearing loss before and after cisplatin-based chemotherapy in testicular cancer survivors: a longitudinal study. Acta Oncologica, 57(8), pp.1075-1083.

Hochman, J.H., Yamazaki, M., Ohe, T. and Lin, J.H., 2002. Evaluation of drug interactions with P-glycoprotein in drug discovery: in vitro assessment of the potential for drug-drug interactions with P-glycoprotein. Current drug metabolism, 3(3), pp.257-273.

Hotamisligil, G.S., and Davis, R.J., 2016. Cell signaling and stress responses. Cold Spring Harbor Perspectives in Biology, 8(10), p.a006072.

Huang, R., Chen, Z., Liu, M., Deng, Y., Li, S. and He, N., 2017. The aptamers generated from HepG2 cells. Science China Chemistry, 60(6), pp.786-792.

Iniguez, E., Sánchez, A., Vasquez, M.A., Martínez, A., Olivas, J., Sattler, A., Sánchez-Delgado, R.A. and Maldonado, R.A., 2013. Metal–drug synergy: new ruthenium (II) complexes of ketoconazole are highly active against Leishmania major and Trypanosoma cruzi and nontoxic to human or murine normal cells. JBIC Journal of Biological Inorganic Chemistry, 18(7), pp.779-790.

Irie, M., Hayakawa, E., Fujimura, Y., Honda, Y., Setoyama, D., Wariishi, H., Hyodo, F. and Miura, D., 2018. Analysis of spatiotemporal metabolomic dynamics for sensitively monitoring biological alterations in cisplatin-induced acute kidney injury. Biochemical and biophysical research communications.

Islam, N. U., Amin, R., Shahid, M., Amin, M., Zaib, S., & Iqbal, J. (2017). A Multi-Target therapeutic potential of Prunus domestica gum stabilized nanoparticles exhibited prospective anticancer, antibacterial, urease-inhibition, anti-inflammatory and analgesic properties. BMC Complementary and Alternative Medicine, 17, 276.

Jamieson, E.R. and Lippard, S.J., 1999. Structure, recognition, and processing of cisplatin− DNA adducts. Chemical Reviews, 99(9), pp.2467-2498.

Ji, Y., Shen, J., Li, M., Zhu, X., Wang, Y., Ding, J., Jiang, S., Chen, L. and Wei, W., 2019. RMP/URI inhibits both intrinsic and extrinsic apoptosis through different signaling pathways. International journal of biological sciences, 15(12), p.2692.

Josefsson, E.C., Burnett, D.L., Lebois, M., Debrincat, M.A., White, M.J., Henley, K.J., Lane, R.M., Moujalled, D., Preston, S.P., O'Reilly, L.A. and Pellegrini, M., 2014. Platelet production proceeds independently of the intrinsic and extrinsic apoptosis pathways. Nature communications, 5, p.3455.

Jungwirth, U., Kowol, C. R., Keppler, B. K., Hartinger, C. G., Berger, W., & Heffeter, P. (2011). Anticancer Activity of Metal Complexes: Involvement of Redox Processes. Antioxidants & Redox Signaling, 15(4), 1085–1127.

Kalyaanamoorthy, S. and Chen, Y.P.P., 2011. Structure-based drug design to augment hit discovery. Drug discovery today, 16(17-18), pp.831-839.

Khan, M.N.I., Staples, R.J., King, C., Fackler Jr, J.P. and Winpenny, R.E., 1993. Syntheses and x-ray structural characterizations of three-coordinate gold (I) and silver (I) complexes with the potentially tetradentate ligand tris (2-(diphenylphosphino) ethyl) amine (NP3):[Au2 (NP3) 2](BPh4) 2, Au (NP3)

PF6, Au (NP3) NO3, Ag (NP3) NO3, and Ag (NP3) PF6. The Au (I) compounds are luminescent. Inorganic Chemistry, 32(25), pp.5800-5807.

Kipps, T.J., Stevenson, F.K., Wu, C.J., Croce, C.M., Packham, G., Wierda, W.G., O'Brien, S., Gribben, J. and Rai, K., 2017. Chronic lymphocytic leukaemia. Nature reviews Disease primers, 3, p.16096.

Kissin, I., 2013. An early indicator of drug success: Top Journal Selectivity Index. Drug design, development and therapy, 7, p.93.

Kletskii, M.E., Burov, O.N., Fedik, N.S. and Kurbatov, S.V., 2017. Thiol-induced NO donation mechanisms in substituted dinitrobenzofuroxans. NO, 62, pp.44-51., M.E., Burov, O.N., Fedik, N.S. and Kurbatov, S.V., 2017. Thiol-induced NO donation mechanisms in substituted dinitrobenzofuroxans. NO, 62, pp.44-51.

Kolch, W., Halasz, M., Granovskaya, M. and Kholodenko, B.N., 2015. The dynamic control of signal transduction networks in cancer cells. Nature Reviews Cancer, 15(9), p.515.

Koliopoulos, G., Nyaga, V.N., Santesso, N., Bryant, A., Martin-Hirsch, P.P., Mustafa, R.A., Schünemann, H., Paraskevaidis, E. and Arbyn, M., 2017. Cytology versus HPV testing for cervical cancer screening in the general population. Cochrane Database of Systematic Reviews, (8).

Koul, A., Arnoult, E., Lounis, N., Guillemont, J. and Andries, K., 2011. The challenge of new drug discovery for tuberculosis. Nature, 469(7331), pp.483-490.

Krishnamoorthy, P., Sathyadevi, P., Cowley, A.H., Butorac, R.R. and Dharmaraj, N., 2011. Evaluation of DNA binding, DNA cleavage, protein binding and in vitro cytotoxic activities of bivalent transition metal hydrazone complexes. European journal of medicinal chemistry, 46(8), pp.3376-3387.

Leijen, S., Burgers, S.A., Baas, P., Pluim, D., Tibben, M., van Werkhoven, E., Alessio, E., Sava, G., Beijnen, J.H. and Schellens, J.H., 2015. Phase I/II study with ruthenium compound NAMI-A and gemcitabine in patients with non-small cell lung cancer after first-line therapy. Investigational new drugs, 33(1), pp.201-214.

Li, P., Mao, Z., Peng, Z., Zhou, L., Chen, Y., Huang, P.H., Truica, C.I., Drabick, J.J., El-Deiry, W.S., Dao, M. and Suresh, S., 2015. Acoustic separation of circulating tumor cells. Proceedings of the National Academy of Sciences, 112(16), pp.4970-4975.

Lipinski, C.A., 2004. Lead-and drug-like compounds: the rule-of-five revolution. Drug Discovery Today: Technologies, 1(4), pp.337-341.

Liu, T., Zeng, L., Jiang, W., Fu, Y., Zheng, W. and Chen, T., 2015. Rational design of cancer-targeted selenium nanoparticles to antagonize multidrug resistance in cancer cells. Nanomedicine: Nanotechnology, Biology and Medicine, 11(4), pp.947-958.

Lücking, U., 2013. Sulfoximines: a neglected opportunity in medicinal chemistry. Angewandte Chemie International Edition, 52(36), pp.9399-9408.

Martelli, M., Vignetti, M., Zinzani, P.L., Gherlinzoni, F., Meloni, G., Fiacchini, M., De Sanctis, V., Papa, G., Martelli, M.F., Calabresi, F. and Tura, S., 1996. High-dose chemotherapy followed by autologous bone marrow transplantation versus

dexamethasone, cisplatin, and cytarabine in aggressive non-Hodgkin's lymphoma with partial response to front-line chemotherapy: a prospective randomized Italian multicenter study. Journal of Clinical Oncology, 14(2), pp.534-542.

Menezo, Y.J., Guerin, J.F. and Czyba, J.C., 1989. Improvement of human early embryo development in vitro by coculture on monolayers of Vero cells. Biology of Reproduction, 42(2), pp.301-306.

Mitra, J., Guerrero, E. N., Hegde, P. M., Wang, H., Boldogh, I., Rao, K. S., … Hegde, M. L. (2014). New Perspectives on Oxidized Genome Damage and Repair Inhibition by Pro-Oxidant Metals in Neurological Diseases. Biomolecules, 4(3), 678–703.

Muller, P.A., and Vousden, K.H., 2013. p53 mutations in cancer. Nature cell biology, 15(1), pp.2-8.

Nama, D., Anil Kumar, P.G. and Pregosin, P.S., 2005. 195Pt, 1H and 31P PGSE diffusion studies on platinum complexes. Magnetic Resonance in Chemistry, 43(3), pp.246-250.

Ndagi, U., Mhlongo, N., & Soliman, M. E. (2017). Metal complexes in cancer therapy – an update from a drug design perspective. Drug Design, Development, and Therapy, 11, 599–616.

Neoh, S.C., Srisukkham, W., Zhang, L., Todryk, S., Greystoke, B., Lim, C.P., Hossain, M.A. and Aslam, N., 2015. An intelligent decision support system for leukaemia diagnosis using microscopic blood images. Scientific Reports, 5, p.14938.

Noyori, R. and Hashiguchi, S., 1997. Asymmetric transfer hydrogenation catalyzed by chiral ruthenium complexes. Accounts of Chemical Research, 30(2), pp.97-102.

O'donoghue, E.J. and Krachler, A.M., 2016. Mechanisms of outer membrane vesicle entry into host cells. Cellular microbiology, 18(11), pp.1508-1517.

Patela, R., Shuklaa, P.K., Vermab, A. and Singhb, M.P., 2016. Pharmacognostical, phytochemical evaluation and insilico lead finding of Callicarpa macrophylla with hepatoprotective potentials. Journal of Chemical and Pharmaceutical Research, 8(3), pp.383-393.

Patridge, E., Gareiss, P., Kinch, M.S. and Hoyer, D., 2016. An analysis of FDA-approved drugs: natural products and their derivatives. Drug discovery today, 21(2), pp.204-207.

Picone, D., Donnarumma, F., Ferraro, G., Gotte, G., Fagagnini, A., Butera, G., Donadelli, M. and Merlino, A., 2017. A comparison study on RNase an oligomerization induced by cisplatin, carboplatin, and oxaliplatin. Journal of inorganic biochemistry, 173, pp.105-112.

Polli, J.W., Wring, S.A., Humphreys, J.E., Huang, L., Morgan, J.B., Webster, L.O. and Serabjit-Singh, C.S., 2001. Rational use of in vitro P-glycoprotein assays in drug discovery. Journal of Pharmacology and Experimental Therapeutics, 299(2), pp.620-628.

Postovit, L.M., Sullivan, R., Adams, M.A., and Graham, C.H., 2005. Nitric oxide signalling and cellular adaptations to changes in oxygenation. Toxicology, 208(2), pp.235-248.

Prabhakaran, R., Kalaivani, P., Jayakumar, R., Zeller, M., Hunter, A.D., Renukadevi, S.V., Ramachandran, E. and Natarajan, K., 2011. Synthesis, structure, and biological evaluation of bis salicylaldehyde-4 (N)-ethylthiosemicarbazone ruthenium (III) triphenylphosphine. Metallomics, 3(1), pp.42-48.

Pérez-Garijo, A. and Steller, H., 2015. Spreading the word: non-autonomous effects of apoptosis during development, regeneration and disease. Development, 142(19), pp.3253-3262.

Petrović, M. and Todorović, D., 2016. Biochemical and molecular mechanisms of action of cisplatin in cancer cells. Facta Universitatis, Series: Medicine & Biology, 18(1).

Prasad, S., Gupta, S.C. and Tyagi, A.K., 2017. Cancer treatment: Role of antioxidative nutraceuticals. Cancer letters, 387, pp.95-105.

Redza-Dutordoir, M. and Averill-Bates, D.A., 2016. Activation of apoptosis signalling pathways by reactive oxygen species. Biochimica et Biophysica Acta (BBA)-Molecular Cell Research, 1863(12), pp.2977-2992.

Rodrigues, A.D., 1997. Preclinical drug metabolism in the age of high-throughput screening: an industrial perspective. Pharmaceutical research, 14(11), pp.1504-1510.

Rosenberg, S. A., Anderson, W. F., Blaese, M., Hwu, P., Yannelli, J. R., Yang, J. C., Ettinghausen, S. E. (1993). The development of gene therapy for the treatment of cancer. Annals of Surgery, 218(4), 455–464.

Reck, M., Rodríguez-Abreu, D., Robinson, A.G., Hui, R., Csőszi, T., Fülöp, A., Gottfried, M., Peled, N., Tafreshi, A., Cuffe, S. and O'Brien, M., 2016. Pembrolizumab versus chemotherapy for PD-L1–positive non–small-cell lung cancer. New England Journal of Medicine, 375(19), pp.1823-1833.

Romeo, G., Ronchetto, P., Luo, Y., Barone, V., Seri, M., Ceccherini, I., Pasini, B., Bocciardi, R., Lerone, M., Kääriäinen, H. and Martucciello, G., 2011. Point mutations affecting the tyrosine kinase domain of the RET proto-oncogene in Hirschsprung's disease. Nature, 367(6461), p.377.

Ryerson, A.B., Eheman, C.R., Altekruse, S.F., Ward, J.W., Jemal, A., Sherman, R.L., Henley, S.J., Holtzman, D., Lake, A., Noone, A.M. and Anderson, R.N., 2016. Annual Report to the Nation on the Status of Cancer, 1975-2012, featuring the increasing incidence of liver cancer. Cancer, 122(9), pp.1312-1337.

Savić, N.D., Milivojevic, D.R., Glišić, B.Đ., Ilic-Tomic, T., Veselinovic, J., Pavic, A., Vasiljevic, B., Nikodinovic-Runic, J. and Djuran, M.I., 2016. A comparative antimicrobial and toxicological study of gold (III) and silver (I) complexes with aromatic nitrogen-containing heterocycles: synergistic activity and improved selectivity index of Au (III)/Ag (I) complexes mixture. RSC advances, 6(16), pp.13193-13206.

Selfors, L.M., Stover, D.G., Harris, I.S., Brugge, J.S. and Coloff, J.L., 2017. Identification of cancer genes that are independent of dominant proliferation and lineage programs. Proceedings of the National Academy of Sciences, 114(52), pp. E11276-E11284.

Serrano, M., Lin, A.W., McCurrach, M.E., Beach, D. and Lowe, S.W., 2014. Oncogenic ras provokes premature cell senescence associated with accumulation of p53 and p16INK4a. Cell, 88(5), pp.593-602.

Simon, H.U., Haj-Yehia, A. and Levi-Schaffer, F., 2000. Role of reactive oxygen species (ROS) in apoptosis induction. Apoptosis, 5(5), pp.415-418.

Sharma, N., Agarwal, D., Gupta, M.K. and Khinchi, M., 2011. A comprehensive review on floating drug delivery system. International Journal of Research in Pharmaceutical and Biomedical Sciences, 2(2), pp.428-441.

Smith, D.A., Di, L. and Kerns, E.H., 2010. The effect of plasma protein binding on in vivo efficacy: misconceptions in drug discovery. Nature reviews Drug discovery, 9(12), pp.929-939.

Srdić-Rajić, T., Zec, M., Todorović, T., Anđelković, K. and Radulović, S., 2011. Non-substituted N-heteroaromatic selenosemicarbazone metal complexes induce apoptosis in cancer cells via activation of the mitochondrial pathway. European journal of medicinal chemistry, 46(9), pp.3734-3747.

Su, Y.C., Davuluri, G.V.N., Chen, C.H., Shiau, D.C., Chen, C.C., Chen, C.L., Lin, Y.S. and Chang, C.P., 2016. Galectin-1-induced autophagy facilitates cisplatin resistance of hepatocellular carcinoma. PLoS One, 11(2), p.e0148408.

Su, Z., Yang, Z., Xu, Y., Chen, Y. and Yu, Q., 2015. Apoptosis, autophagy, necroptosis, and cancer metastasis. Molecular cancer, 14(1), p.48.

Sun, Y., Liu, W.Z., Liu, T., Feng, X., Yang, N. and Zhou, H.F., 2015. Signaling pathway of MAPK/ERK in cell proliferation, differentiation, migration, senescence, and apoptosis. Journal of Receptors and Signal Transduction, 35(6), pp.600-604.

Suresh, S., Girija, C.R., Sathish, C.D. and Venkatesha, T.V., 2016. Schiff Base N-(5-Chlorosalicylidene) Aniline, a Novel Antifungal Agent: Insights from Crystallographic Analysis, Semi Empirical and Molinspirations Calculations. Chem Sci J, 7, p.122.

Thanan, R., Oikawa, S., Hiraku, Y., Ohnishi, S., Ma, N., Pinlaor, S., Yongvanit, P., Kawanishi, S. and Murata, M., 2015. Oxidative stress and its significant roles in neurodegenerative diseases and cancer. International journal of molecular sciences, 16(1), pp.193-217.

Theon, A.P., Pascoe, J.R., Carlson, G.P. and Krag, D.N., 1993. Intratumoral chemotherapy with cisplatin in the oily emulsion in horses. Journal of the American Veterinary Medical Association, 202(2), pp.261-267.

Tomás-Gamasa, M., Martínez-Calvo, M., Couceiro, J.R. and Mascareñas, J.L., 2016. Transition metal catalysis in the mitochondria of living cells. Nature communications, 7, p.12538.

Tzeng, B.C., Liao, J.H., Lee, G.H. and Peng, S.M., 2004. Photophysical properties, electronic and crystal structures of luminescent diphosphine digold (I)-pyridine-2-thiolate complexes. Inorganica chimica acta, 357(5), pp.1405-1410.

Valko, M., Rhodes, C., Moncol, J., Izakovic, M.M. and Mazur, M., 2006. Free radicals, metals, and antioxidants in oxidative stress-induced cancer. Chemical-biological interactions, 160(1), pp.1-40.

Van Dam, D. and De Deyn, P.P., 2011. Animal models in the drug discovery pipeline for Alzheimer's disease. British journal of pharmacology, 164(4), pp.1285-1300.

Van de Bunt, L., Van der Heide, U.A., Ketelaars, M., de Kort, G.A. and Jürgenliemk-Schulz, I.M., 2006. Conventional, conformal, and intensity-modulated radiation therapy treatment planning of external beam radiotherapy for cervical cancer: The impact of tumour regression. International Journal of Radiation Oncology* Biology* Physics, 64(1), pp.189-196.

Van der Greef, J. and McBurney, R.N., 2005. Rescuing drug discovery: in vivo systems pathology and systems pharmacology. Nature Reviews Drug Discovery, 4(12), pp.961-967.

Vilar, S., Cozza, G. and Moro, S., 2008. Medicinal chemistry and the molecular operating environment (MOE): application of QSAR and molecular docking to drug discovery. Current topics in medicinal chemistry, 8(18), pp.1555-1572.

Vineis, P. and Wild, C.P., 2014. Global cancer patterns cause and prevention. The Lancet, 383(9916), pp.549-557.

Webb, M.I., Chard, R.A., Al-Jobory, Y.M., Jones, M.R., Wong, E.W. and Walsby, C.J., 2011. Pyridine analogs of the antimetastatic Ru (III) complex NAMI-A targeting non-covalent interactions with albumin. Inorganic chemistry, 51(2), pp.954-966.

Weiming, X.U., Liu, L.Z., Loizidou, M., Ahmed, M. and Charles, I.G., 2002. The role of nitric oxide in cancer. Cell research, 12(5), pp.311-320.

Weinstein, I.B. and Joe, A.K., 2006. Mechanisms of disease: oncogene addiction—a rationale for molecular targeting in cancer therapy. Nature Reviews Clinical Oncology, 3(8), p.448.

Wendehenne, D., Durner, J. and Klessig, D.F., 2004. Nitric oxide: a new player in plant signalling and defence responses. Current opinion in plant biology, 7(4), pp.449-455.

Wenzel, M., Bertrand, B., Eymin, M.J., Comte, V., Harvey, J.A., Richard, P., Groessl, M., Zava, O., Amrouche, H., Harvey, P.D., and Le Gendre, P., 2011. Multinuclear cytotoxic metallodrugs: physicochemical characterization and biological properties of novel heteronuclear gold–titanium complexes. Inorganic chemistry, 50(19), pp.9472-9480.

Wienkers, L.C. and Heath, T.G., 2005. Predicting in vivo drug interactions from in vitro drug discovery data. Nature reviews Drug discovery, 4(10), pp.825-833.

Wishart, D.S., 2007. Improving early drug discovery through ADME modelling. Drugs in R & D, 8(6), pp.349-362.

Wright, T.C., Stoler, M.H., Behrens, C.M., Sharma, A., Zhang, G., and Wright, T.L., 2015. Primary cervical cancer screening with human papillomavirus: end of study results from the ATHENA study using HPV as the first-line screening test. Gynecologic oncology, 136(2), pp.189-197.

Wu, Y.J., Su, T.R., Dai, G.F., Su, J.H. and Liu, C.I., 2019. Flaccidoxide-13-Acetate-Induced Apoptosis in Human Bladder Cancer Cells is through Activation of p38/JNK, Mitochondrial Dysfunction, and Endoplasmic Reticulum Stress Regulated Pathway. Marine drugs, 17(5), p.287.

Yang, J., Liu, X., Bhalla, K., Kim, C.N., Ibrado, A.M., Cai, J., Peng, T.I., Jones, D.P. and Wang, X., 1997. Prevention of apoptosis by Bcl-2: release of cytochrome c from mitochondria blocked. Science, 275(5303), pp.1129-1132.

Zeng, S., Zhang, H., Ding, Z., Luo, R., An, K., Liu, L., Bi, J., Chen, H., Xiao, S. and Fang, L., 2015. Proteome analysis of porcine epidemic diarrhea virus (PEDV) -infected Vero cells. Proteomics, 15(11), pp.1819-1828.

Zeng, Q., Lewis, F.W., Harwood, L.M. and Hartl, F., 2015. Role of ligands in catalytic water oxidation by mononuclear ruthenium complexes. Coordination Chemistry Reviews, 304, pp.88-101.

Zhang, Z., Kong, F., Ni, H., Mo, Z., Wan, J.B., Hua, D. and Yan, C., 2016. Structural characterization, α-glucosidase inhibitory and DPPH scavenging activities of polysaccharides from guava. Carbohydrate polymers, 144, pp.106-114.

Zhu, H., Luo, H., Zhang, W., Shen, Z., Hu, X. and Zhu, X., 2016. Molecular mechanisms of cisplatin resistance in cervical cancer. Drug design, development and therapy, 10, p.1885.

CHAPTER 7: APPENDIX

1.15 Appendix I: List of reagents and company information

The following Reagents were used in this study

Table A1: Information of reagents used in the study

Reagent	Catalogue number	Company	Country
DMEM Media	41966029	Sigma-Aldrich	USA
HEPES Buffer	15630056	Gibco, Life Technologies	USA
Sodium Pyruvate	SH30239.01	Hyclone, Thermo scientific	USA
Gentamicin	G1272-10ML	Sigma-Aldrich	USA
Foetal-Bovine Serum	10270106	Gibco, Life Technologies	USA
Trypsin-EDTA	T4049-500ML	Sigma-Aldrich	UK
RPMI Media	R6504-10X1L	Sigma-Aldrich	USA
Antibiotic/Antimitotic	SV30079.01	Separations	SA
Thiazol Blue Tetrazolium Bromide (MTT)	M5655-1G	Sigma-Aldrich	GER
Auranofin	A6733	Sigma-Aldrich	GER
MEM Media	SH30024.01	Separations	SA
DMSO	D2650-100ML	Sigma-Aldrich	GER

The following instrumentation software programs were used in the study

Table A2: List of important instruments used in the study

Instrumentation	Company	Country
Allegra 25R centrifuge	Beckman Coulter	USA
Multiskan Ascent plate reader	Thermo Lab Systems	USA
BD Accuri™ C6 Plus flow cytometer	Accuri Cytometers Inc.	USA

Table A3: Software programs used for data analysis

Program	Company	Country
Chemsketch Freeware version 11.01	Advanced Chemistry Development Inc.	Canada
GraphPad Prism 5	GraphPad Software Inc.	USA
Microsoft Excel 365	Microsoft Corporation	USA
Molinspiration Freeware	Molinspiration	USA

1.16 Appendix II: Formulae for Data Analysis

Formula 1: Calculating cell concentration using a haemocytometer:

$$\text{Cell Concentration} = \left(\frac{Total\ live\ cells}{Number\ of\ squares}\right) \times Dilution\ \times 10^4$$

Formula 2: Calculating cell viability

$$\%\ Viability = \left(\frac{(Ave\ complex\ abosrbance)-(Ave\ blank\ absorbance)}{(Ave\ untreated\ cell\ absorbance)-(Ave\ blank\ absorbance)}\right)\times 100$$

% Cytotoxicity = 100-%Viability

Formula 3: Calculating selectivity index (SI)

$$\text{SI} = \frac{CC50\ Normal\ cell}{CC50\ cancer\ cell}$$

Formula 4: Calculating DPPH scavenging activity

$$\%\ \text{Scavenging} = \left(A_0 - \frac{A_0}{A_S}\right)\times 100$$

Where A_0 is the average absorbance of the DPPH only control and A_S is the average absorbance of DPPH in the presence of each metal complex.

Formula 5: Student's T-test for statistical significance

$$t = \frac{M_x - M_y}{\sqrt{\frac{S_x^{\,2}}{n_x} + \frac{S_y^{\,2}}{n_y}}}$$

M = mean
n = number of scores per group

$$S^2 = \frac{\sum (x - M)^2}{n - 1}$$

x = individual scores
M = mean
n= number of scores in group

1.17 Appendix III: Cell Viability

The metal complexes exhibited the following effects on the growth of HeLa cells. These results were used to calculate the CC_{50} values.

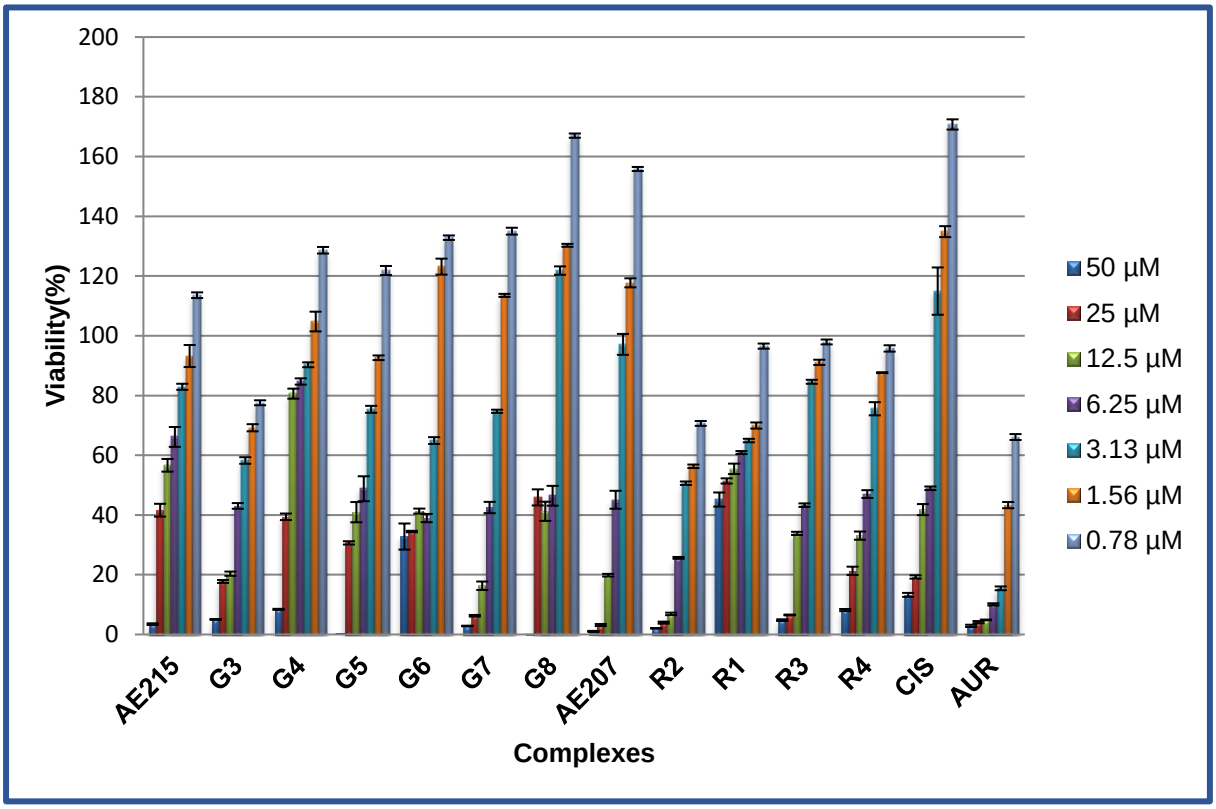

Figure A1: HeLa cell viability. The above figure shows the HeLa cell viability after treatments with the metal complexes. There was a dosage response when the tested concentration increased from 0.78 um to 50 um with a decrease in cell viability when we increased the complex concentration. The ruthenium complexes were more cytotoxic than the gold complexes. N=4, ±SEM

The metal complexes were then treated on HepG2 cells and their cell viability were shown in the figure below.

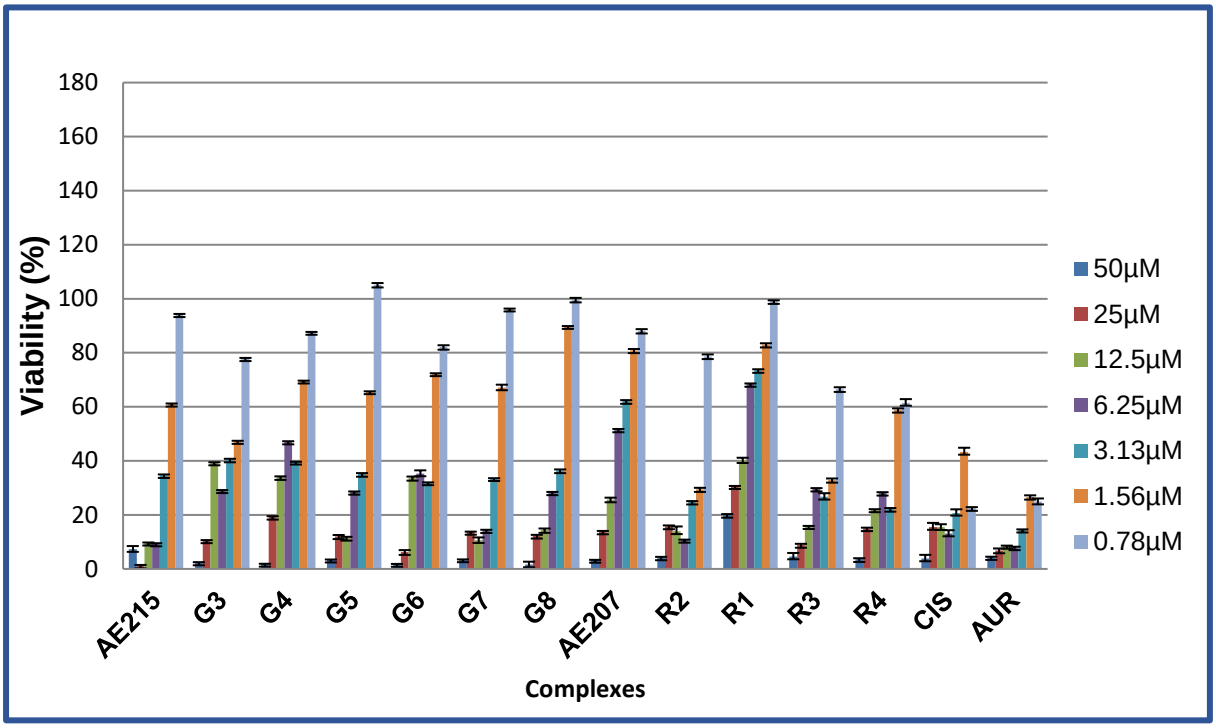

Figure A2: U937 Cell Viability. The above figure shows the cell viability after treating U937 cells with the complexes for 72 hours. After treatments, we observed that the complexes were quite toxic to this cell line with viabilities of just under 100% for all tested concentrations. N=4, ±SEM

Lastly, we treated the HepG2 cells with the complexes then we recorded the results in the figure below.

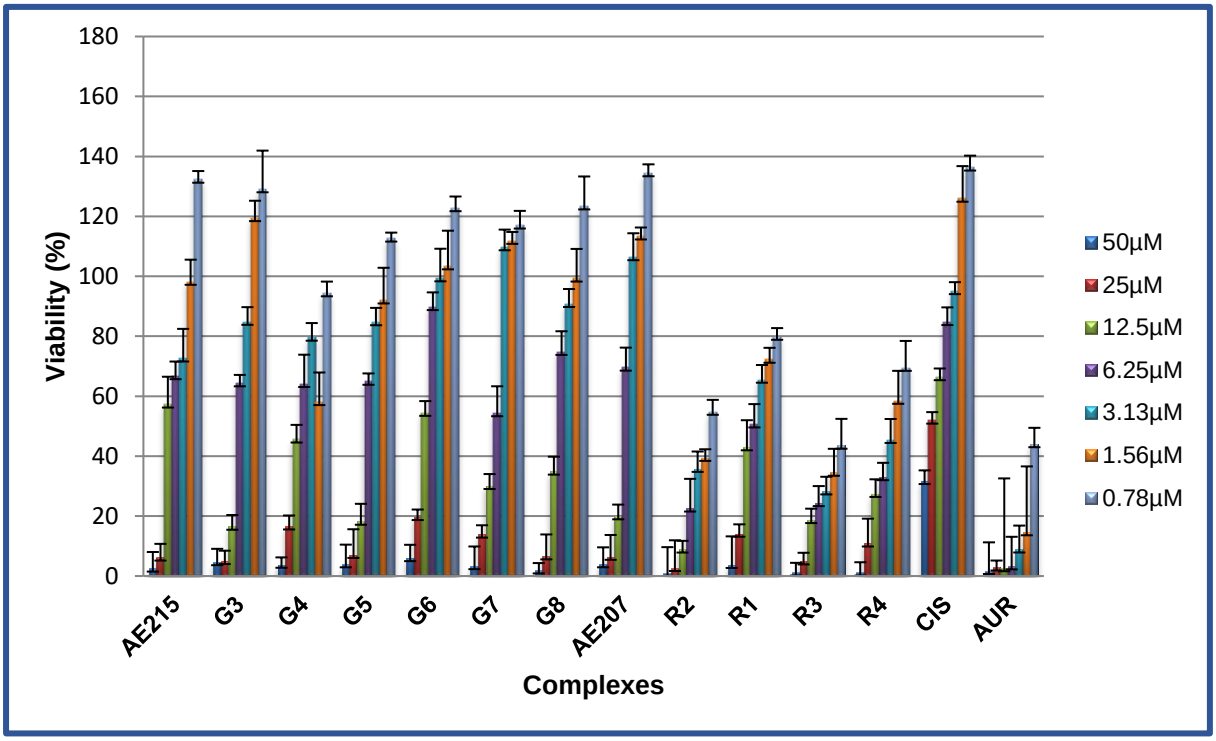

Figure A4 HepG2 cell viability. The above-figure indicates HepG2 cell viability in the presence of the complexes. The complexes were less cytotoxic in this cell line compared to HeLa cells. Treatments were for 72 hours and we saw that the ruthenium complexes were more toxic than the gold complexes. N=4, ±SEM

Appendix v: Apoptosis induction

The active metal complexes were tested for their apoptosis-inducing abilities. We saw that all of these complexes were able to induce apoptosis in all cell lines. The untreated controls showed that when cells were not treated they were still live after 72 hours. The ruthenium complexes induced the most apoptosis across all cell lines.

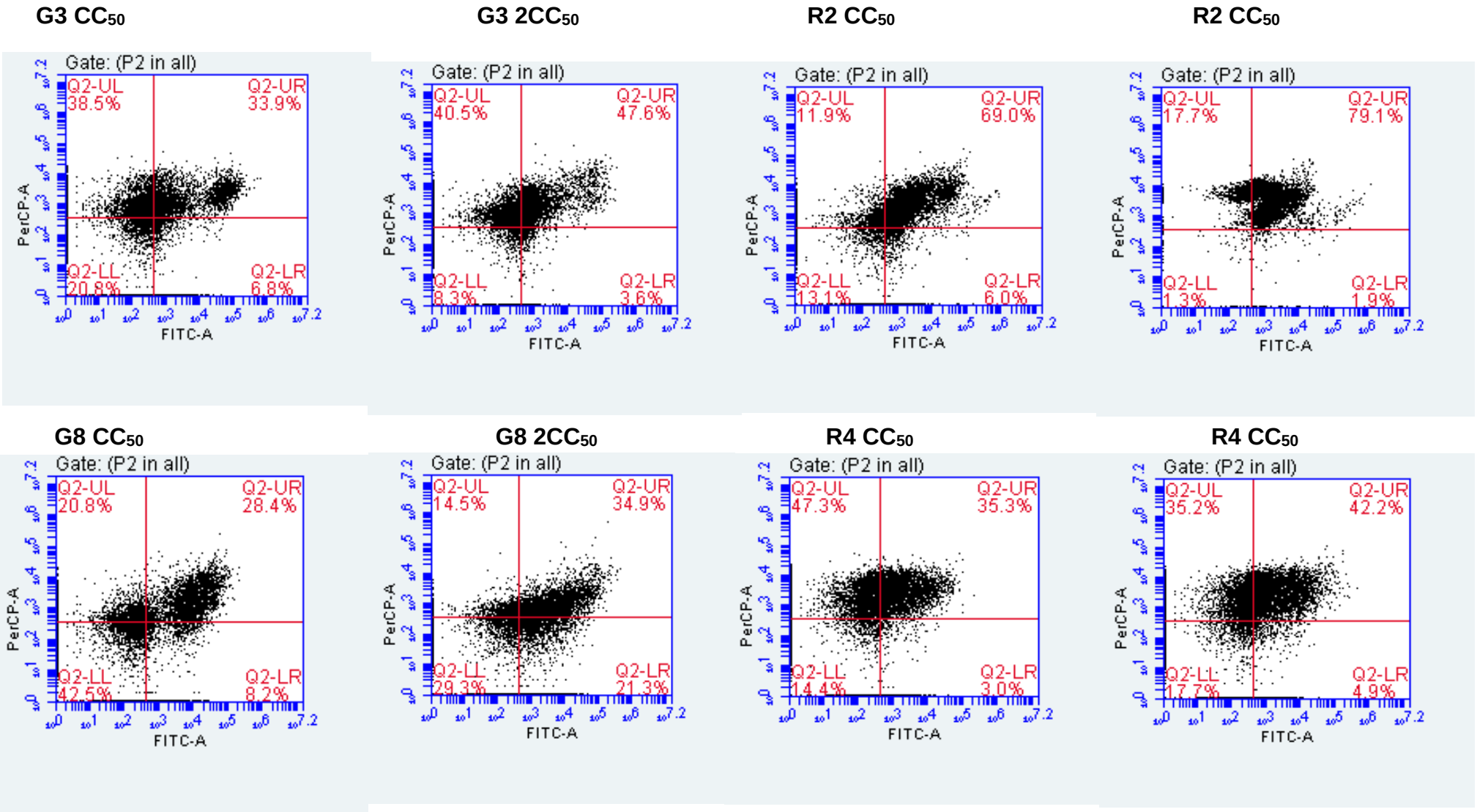

Figure 12: HeLa apoptosis-induction. *The above images show flow cytometry data obtained from treating HeLa cells* ***G3, G8, R2*** *and* ***R4*** *complexes at the* CC_{50} *and* $2CC_{50}$. *All complexes were able to induce apoptosis at both tested concentrations.* ***G8*** *was unable to induce apoptosis at both tested concentrations.* ***R2*** *was able to induce apoptosis to over 70% at* $2CC_{50}$.

7.1 Contour diagrams of FITC-Annexin V/PI flow cytometry of treatments on U937 cells

Controls

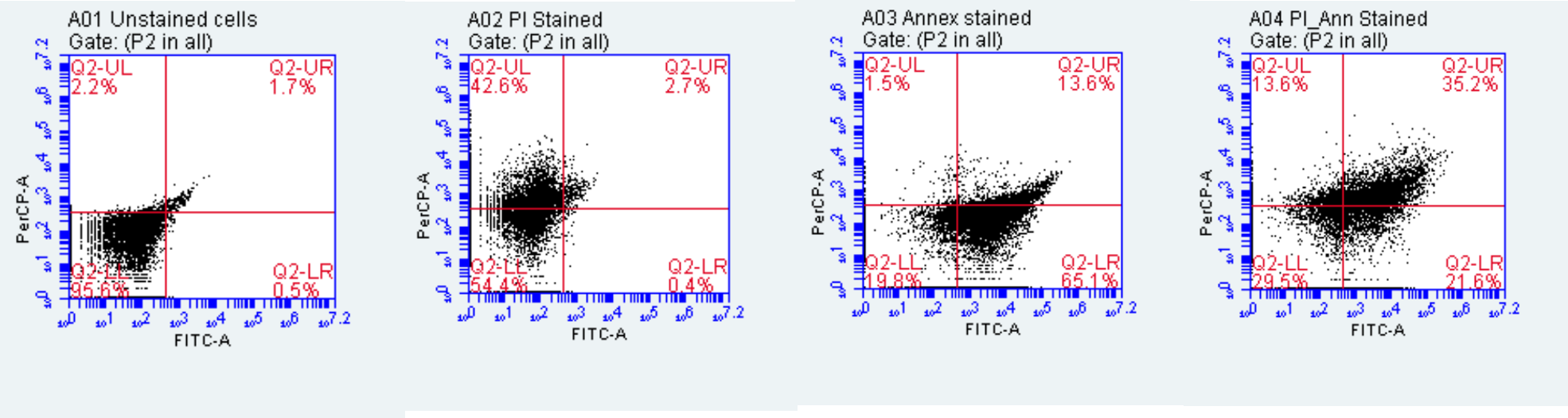

***Figure 13: The above image shows Flow cytometry data of the tested complexes on U937 cells**. The same controls were used.*

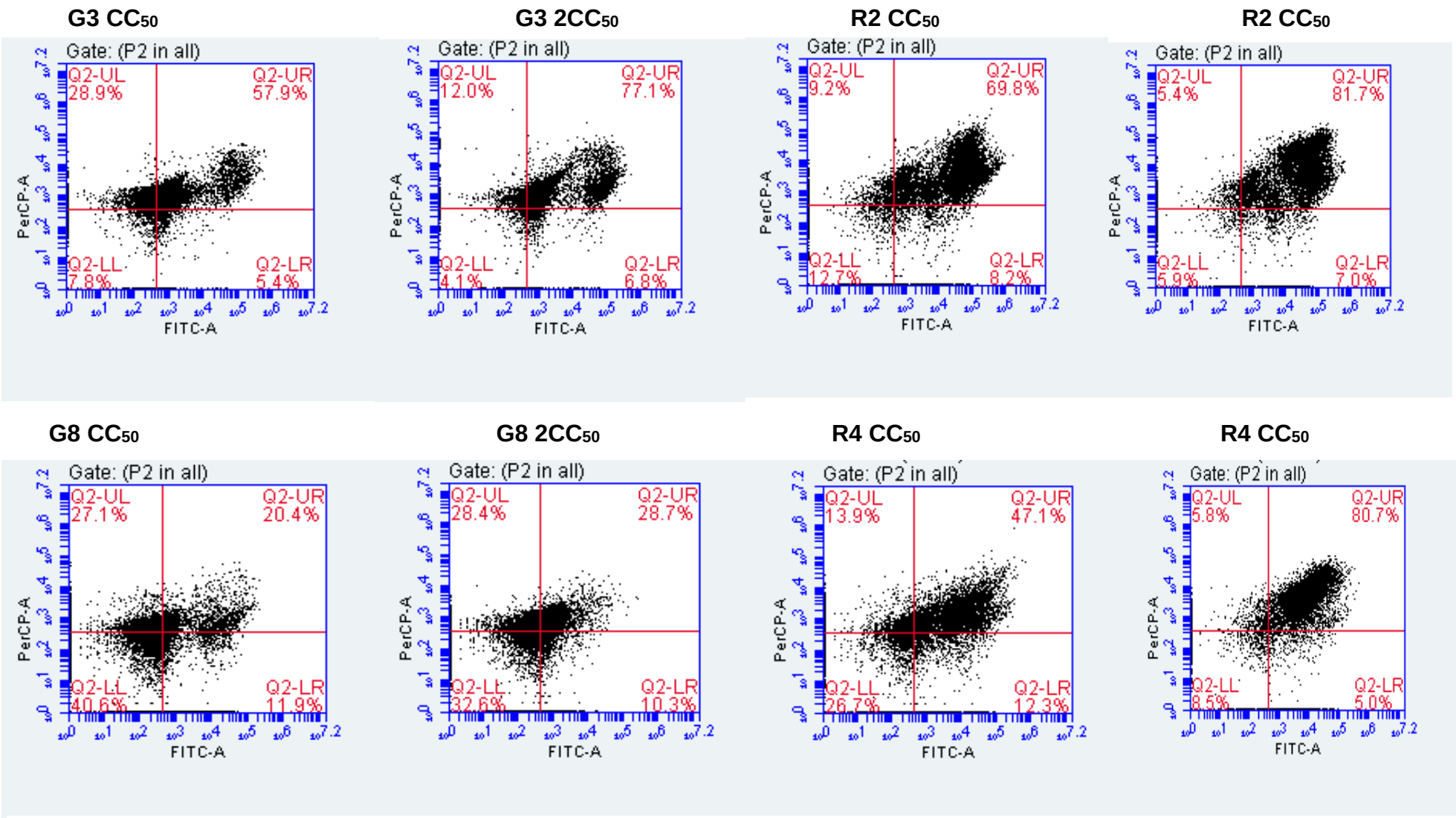

Figure 14: Flow cytometry plots obtained from U937 cells*. The above image shows the data obtained after treating the cells with the active metal complexes for 72 hours and staining them with PI and Annexin V. All complexes were able to induce apoptosis where* ***G3, R2, R4*** *were able to induce apoptosis to over 70%.*

7.2 Contour diagrams of FITC-Annexin V/PI flow cytometry of treatments on HepG2 cells

Controls

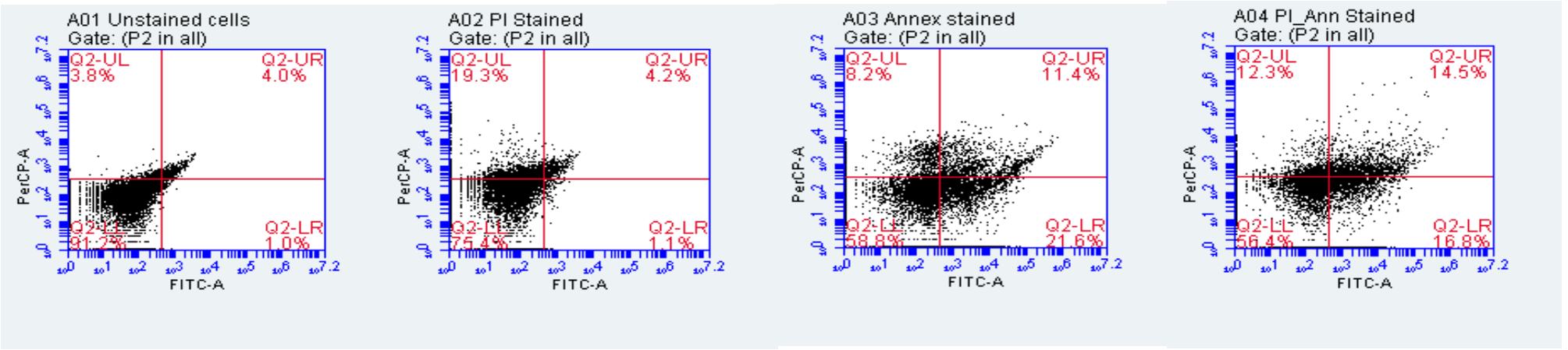

***Figure 15: HepG2 flow cytometry control data**. The above image shows the data obtained from staining the cells with PI, Annexin V, and PI+ Annexin V. There is no clear difference between untreated and PI-stained cells compared to the previous cell lines.*

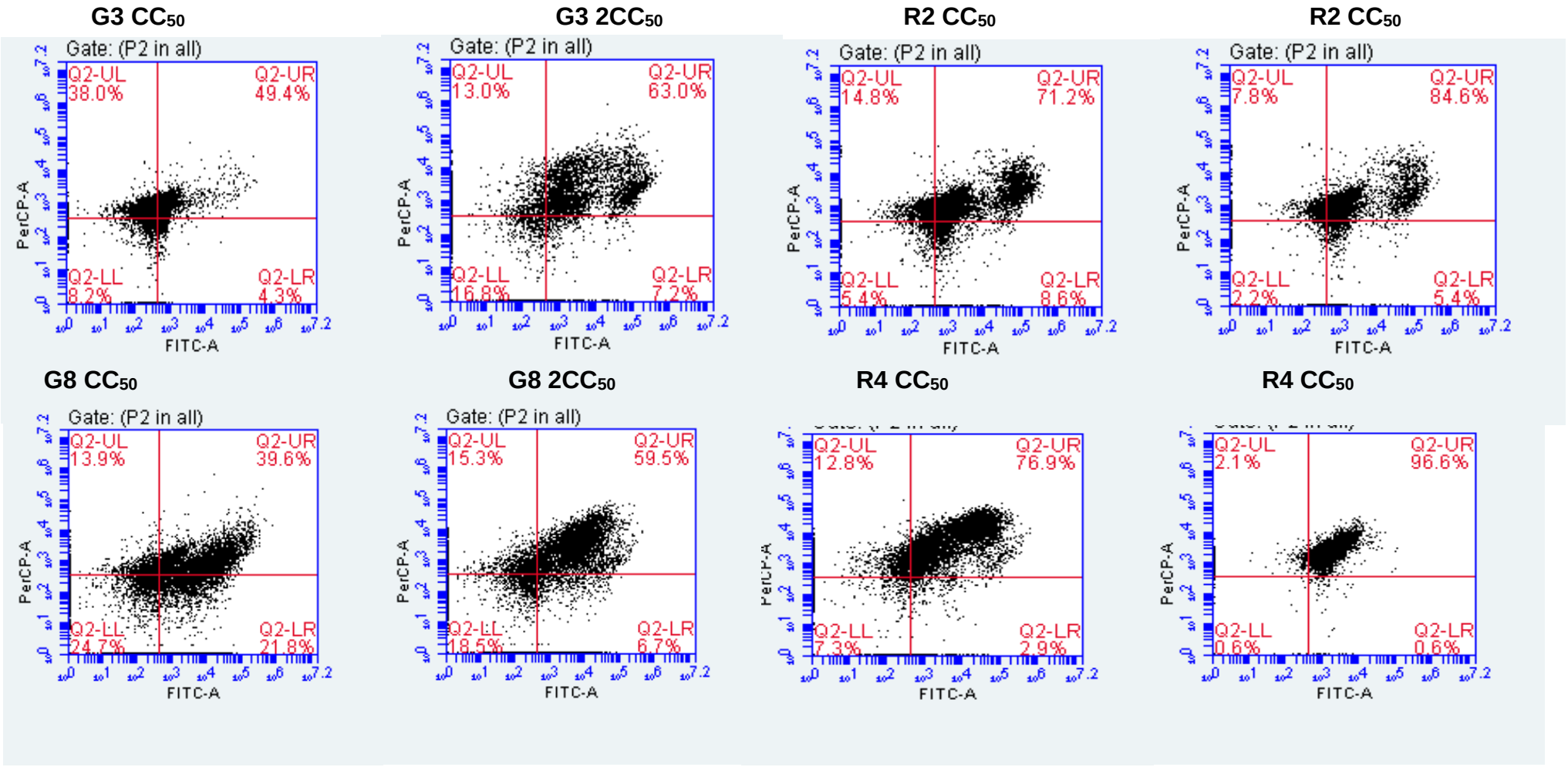

***Figure 16:HepG2 flow cytometry data**. The above image shows the results obtained from treating the cell line with the active complexes at CC_{50} and $2XCC_{50}$. Only **G3** was able to induce apoptosis over 60% compared to other complexes. N=4.*

`